Table 2 The associations between baseline chemokine levels and subsequent clinical parameters in patients with SSc

	Baseline	1 year follow-up	2 year follow-up	3 year follow-up	4 year follow-up
Baseline CCL2 versus MRSS (baseline–4 years)	$r = 0.16$, $P = 0.36$	$r = 0.43$, $P = 0.013$	$r = 0.21$, $P = 0.25$	$r = 0.10$, $P = 0.56$	$r = 0.19$, $P = 0.29$
Baseline CCL2 versus %VC (baseline–4 years)	$r = -0.24$, $P = 0.23$	$r = -0.13$, $P = 0.67$	$r = -0.40$, $P = 0.079$	$r = -0.32$, $P = 0.15$	$r = -0.31$, $P = 0.14$
Baseline CCL2 versus HAQ-DI (baseline–4 years)	$r = 0.44$, $P = 0.011$	$r = 0.56$, $P = 0.0007$	$r = 0.52$, $P = 0.0019$	$r = 0.42$, $P = 0.014$	$r = 0.49$, $P = 0.0040$
Baseline CCL5 versus MRSS (baseline–4 years)	$r = 0.21$, $P = 0.25$	$r = 0.023$, $P = 0.90$	$r = 0.019$, $P = 0.92$	$r = 0.12$, $P = 0.51$	$r = 0.11$, $P = 0.54$
Baseline CCL5 versus %VC (baseline–4 years)	$r = -0.090$, $P = 0.66$	$r = -0.26$, $P = 0.39$	$r = -0.085$, $P = 0.72$	$r = -0.14$, $P = 0.54$	$r = -0.23$, $P = 0.27$
Baseline CCL5 versus HAQ-DI (baseline–4 years)	$r = 0.056$, $P = 0.76$	$r = -0.11$, $P = 0.56$	$r = -0.11$, $P = 0.95$	$r = 0.013$, $P = 0.94$	$r = -0.076$, $P = 0.68$
Baseline CXCL8 versus MRSS (baseline–4 years)	$r = -0.053$, $P = 0.77$	$r = 0.40$, $P = 0.021$	$r = 0.16$, $P = 0.39$	$r = 0.035$, $P = 0.85$	$r = 0.14$, $P = 0.44$
Baseline CXCL8 versus %VC (baseline–4 years)	$r = -0.081$, $P = 0.69$	$r = -0.21$, $P = 0.48$	$r = -0.14$, $P = 0.56$	$r = -0.010$, $P = 0.96$	$r = 0.0052$, $P = 0.98$
Baseline CXCL8 versus HAQ-DI (baseline–4 years)	$r = 0.47$, $P = 0.0009$	$r = 0.72$, $P < 0.0001$	$r = 0.74$, $P < 0.0001$	$r = 0.48$, $P = 0.0044$	$r = 0.45$, $P = 0.0081$
Baseline CXCL9 versus MRSS (baseline–4 years)	$r = -0.23$, $P = 0.24$	$r = -0.068$, $P = 0.71$	$r = -0.26$, $P = 0.14$	$r = -0.35$, $P = 0.042$	$r = -0.31$, $P = 0.082$
Baseline CXCL9 versus %VC (baseline–4 years)	$r = -0.13$, $P = 0.48$	$r = -0.004$, $P = 0.99$	$r = -0.25$, $P = 0.29$	$r = -0.37$, $P = 0.093$	$r = -0.29$, $P = 0.17$
Baseline CXCL9 versus HAQ-DI (baseline–4 years)	$r = 0.18$, $P = 0.31$	$r = 0.10$, $P = 0.58$	$r = 0.016$, $P = 0.93$	$r = 0.093$, $P = 0.61$	$r = 0.053$, $P = 0.77$
Baseline CXCL10 versus MRSS (baseline–4 years)	$r = -0.055$, $P = 0.76$	$r = -0.16$, $P = 0.38$	$r = -0.21$, $P = 0.25$	$r = -0.31$, $P = 0.082$	$r = -0.23$, $P = 0.21$
Baseline CXCL10 versus %VC (baseline–4 years)	$r = -0.045$, $P = 0.82$	$r = 0.16$, $P = 0.59$	$r = 0.17$, $P = 0.47$	$r = -0.28$, $P = 0.20$	$r = -0.23$, $P = 0.27$
Baseline CXCL10 versus HAQ-DI (baseline–4 years)	$r = 0.20$, $P = 0.27$	$r = 0.080$, $P = 0.66$	$r = -0.045$, $P = 0.80$	$r = -0.11$, $P = 0.53$	$r = -0.040$, $P = 0.82$

Table 3 Factors predicting HAQ-DI of 4 year follow-up determined by multiple regression analysis

	Estimate	Standard error	*P* value
Intercept	−0.24	0.49	0.63
Log_{10} (serum CXCL8 levels of baseline) pg/ml	0.81	0.23	0.0016
%VC of baseline	−0.0061	0.0033	0.086

The multiple regression equations predicting HAQ-DI of 4 year follow-up are as follows; HAQ-DI of 4 year follow-up = $-0.24 + 0.81 \times \log_{10}$ [serum CXCL8 levels (pg/ml) of baseline] + $-0.0061 \times$ %VC of baseline. R^2 (determination coefficient) = 0.41, root mean square error = 0.36, $P = 0.0016$

Discussion

In this study, we measured serum chemokine levels using a cytometric beads array, a method that has comparable analytical sensitivity, but a wider dynamic range than conventional ELISA [17]. Serum levels of CCL2, CCL5, CXCL8, CXCL9, and CXCL10 were significantly elevated in early SSc patients with diffuse skin sclerosis and/or ILD. In this multicenter, longitudinal, prospective study, a multiple regression equation was defined to predict symptoms 4 years after initial diagnosis using baseline serum levels of five chemokines and multiple clinical or laboratory factors presenting at the time of the first visit. In this regard, we found that the initial serum CXCL8 levels were significantly associated with the HAQ-DI at the fourth year while the %VC of baseline tended to be negatively associated with HAQ-DI at the fourth year.

CXCL8 is a member of the CXC chemokine family which has an ELR (glutamic acid–leucine–arginine) motif between the N-terminus and the first cysteine that attracts CXCL1- or CXCL2-expressing neutrophils [18]. Of note, CXCL8 gene polymorphisms are associated with an

increased risk of SSc [19] and elevated serum CXCL8 levels have been reported in SSc patients [20, 21]. A recent study demonstrated that plasma CXCL8 levels are specifically elevated in SSc patients with anti-topoisomerase I Ab [22]. Furthermore, expression levels of CXCL8 are increased in skin biopsy specimens from patients with SSc, especially patients with early SSc [23]. SSc dermal fibroblasts produce more CXCL8 than do fibroblasts from healthy controls in vitro [24]. CXCL8 is also increased in bronchoalveolar lavage (BAL) fluid from patients with SSc, suggesting a critical role for CXCL8 in ILD of SSc patients [25–27]. Taken together, elevated serum levels of CXCL8 measured in early SSc patients in our study are consistent with previous reports.

We found that baseline serum CXCL8 levels were significantly associated with severity of physical dysfunction at the baseline and subsequent years. Since serum CXCL8 levels were not significantly associated with specific organ involvement, CXCL8 may affect neutrophil infiltration into various organs, resulting in systemic inflammation and subsequent functional disability. In addition, endothelial cell activation has been considered a first step in the development of tissue fibrosis [2], and CXCL8 is synthesized by endothelial cells, which store this chemokine in storage vesicles known as Weibel–Palade bodies [28, 29]. Therefore, it is interesting that baseline serum CXCL8 levels were associated more closely with HAQ-DI of the first and second year compared with baseline HAQ-DI.

CCL2 is produced by monocytes, fibroblasts, endothelial cells and other cells, and is a predominant chemoattractant and activator of monocytes and T cells [18]. Increased CCL2 expression on SSc fibroblasts stimulates the chemotaxis of mononuclear cells [30]. In addition to its chemoattractant activities, CCL2 induces Th2 cell polarization and stimulates collagen production by fibroblasts via endogenous upregulation of TGF-β expression [31–33]. CCR2, the receptor for CCL2, is upregulated in the skin of patients with active SSc and CCR2 expression on SSc fibroblasts appears to positively regulate the expression of CCL2 and α-smooth muscle actin [34]. In the current study serum CCL2 levels were found to be increased, consistent with previous reports [35, 36], and the baseline CCL2 levels were significantly associated with HAQ-DI at baseline and subsequent every year until 4 years by univariate analysis. However, baseline CCL2 levels were not significantly associated HAQ-DI at the fourth year as determined by multiple regression analysis.

There are some discrepancies between the findings in this study and the results of our previous study [37]. In the previous study, we analyzed serum chemokine levels in Japanese early SSc patients of single center during 3 years. Although CXCL8 levels tended to be higher in patients than in controls at their first visit, the difference was not statistically significant. Levels of CCL2, CXCL9, and CXCL10 were significantly increased consistent with the current findings, although CCL5 were not measured in that study. Since the measuring procedures and measurers were the same in both studies, the difference is likely to due the difference of population. Previous study included only 31 patients of a single center. On the other hand, 70 non-overlapping patients of multicenter were examined in this study and this made it possible to detect a significant increase of CXCL8 in patients with SSc. Although the variations of CCL2 were significantly associated with the variations of skin thickness score and VC during 3 years in our previous study, we could not detect those findings in this study. Our current findings together with the previous results indicate that CXCL8 in addition to CCL2 are candidates of biomarkers in SSc.

In this study, serum CXCL8 levels strongly correlated with serum CCL2 levels at the patients' first visit. In general, CXCL8 and CCL2 are the most critical chemokines for the recruitment of neutrophils and monocytes, respectively. Further, the transition from neutrophil to monocyte accumulation during inflammation might be linked to a shift in chemokine synthesis from CXCL8 to CCL2, probably via IL-6 signaling [38]. Therefore, increased CXCL8 production may trigger initial inflammation while CCL2 may contribute to the subsequent chronic inflammation and fibrosis in SSc. Thus, CXCL8 levels, rather than CCL2 levels, can likely predict the progression of SSc, despite the finding that serum levels of CXCL8 and CCL2 were associated with each other.

CCL5 produced by T cells and other cell types is chemotactic for T cells and eosinophils [18]. Abundant expression of the mRNA and elevated protein levels of CCL5 have been detected in the skin of SSc patients, but not in the skin of healthy controls [39, 40]. Moreover, levels of CCL5 are increased in BAL fluids from SSc patients [26]. Although serum CCL5 levels in SSc patients have been reported to be comparable to those of healthy controls [41], the levels of CCL5 were found to be significantly elevated in early SSc patients in this study. Since our patients were selected as those with early SSc with diffuse skin sclerosis and/or ILD, it is likely that serum CCL5 is elevated in these active patients.

CXCL9 and CXCL10 belong to the family of CXC chemokines without an ELR motif and chemoattract CXCR3-expressed Th1 cells. These chemokines are produced by numerous cell types in response to IFN-γ, including monocytes and epithelial cells [18]. Serum levels of both CXCL9 and CXCL10 are reportedly increased in SSc patients compared to controls [36, 42, 43]. In one study, high values of CXCL10 were associated with a more severe clinical phenotype that was characterized by lung and kidney involvement [36]. Although our patients with

early SSc also showed significantly elevated CXCL9 and CXCL10 levels, the levels did not correlate with clinical features in our selected population.

Some limitations exist in this study including analysis of a relatively small population size as well as the fact that this is an observational study and, therefore, the treatment protocol is heterogeneous. Nonetheless, our data indicate that serum CXCL8 levels may be useful for predicting the decline in physical function in patients with progressive SSc. Further longitudinal studies in a larger population will clarify the utility of serum chemokine levels as prognostic indicators in SSc patients.

Acknowledgments The manuscript has not been previously published nor has it been submitted simultaneously for publication elsewhere. We are grateful to all the physicians who have contributed to data collection at each facility. We also thank Tomoko Hayashi, Yuko Yamada, and Masako Matsubara for their assistance in registering data. This work was supported by funds for research on intractable diseases from the Ministry of Health, Labor, and Welfare of Japan.

References

1. Gabrielli A, Avvedimento EV, Krieg T. Scleroderma. N Engl J Med. 2009;360(19):1989–2003.
2. Bhattacharyya S, Wei J, Varga J. Understanding fibrosis in systemic sclerosis: shifting paradigms, emerging opportunities. Nat Rev Rheumatol. 2012;8(1):42–54.
3. Roumm AD, Whiteside TL, Medsger TA Jr, Rodnan GP. Lymphocytes in the skin of patients with progressive systemic sclerosis. Quantification, subtyping, and clinical correlations. Arthritis Rheum. 1984;27(6):645–53.
4. Gruschwitz M, Sepp N, Kofler H, Wick G. Expression of class II-MHC antigens in the dermis of patients with progressive systemic sclerosis. Immunobiology. 1991;182(3–4):234–55.
5. Atamas SP, White B. The role of chemokines in the pathogenesis of scleroderma. Curr Opin Rheumatol. 2003;15(6):772–7.
6. Hasegawa M, Sato S. The roles of chemokines in leukocyte recruitment and fibrosis in systemic sclerosis. Front Biosci. 2008; 13:3637–47.
7. Steen VD, Medsger TA Jr. Severe organ involvement in systemic sclerosis with diffuse scleroderma. Arthritis Rheum. 2000;43(11): 2437–44.
8. Medsger TA Jr. Classification, purpose. In: Clements PJ, Furst DE, editors. Systemic sclerosis. Philadelphia: Williams & Wilkins; 2004. p. 17–28.
9. Steen VD. Autoantibodies in systemic sclerosis. Semin Arthritis Rheum. 2005;35(1):35–42.
10. Lit LC, Wong CK, Tam LS, Li EK, Lam CW. Raised plasma concentration and ex vivo production of inflammatory chemokines in patients with systemic lupus erythematosus. Ann Rheum Dis. 2006;65(2):209–15.
11. Bauer JW, Petri M, Batliwalla FM, Koeuth T, Wilson J, Slattery C, et al. Interferon-regulated chemokines as biomarkers of systemic lupus erythematosus disease activity: a validation study. Arthritis Rheum. 2009;60(10):3098–107.
12. LeRoy EC, Krieg T, Black C, Medsger TAJ, Fleischmajer R, Rowell N, et al. Scleroderma (systemic sclerosis): classification, subsets, and pathogenesis. J Rheumatol. 1988;15:202–5.
13. Subcommittee for Scleroderma Criteria of the American Rheumatism Association Diagnostic and Therapeutic Criteria Committee. Preliminary criteria for the classification of systemic sclerosis (scleroderma). Arthritis Rheum. 1980;23:581–90.
14. Clements P, Lachenbrush P, Seibold J, White B, Weiner S, Martin R, et al. Inter and intraobserver variability of total skin thickness score (modified Rodnan TSS) in systemic sclerosis. J Rheumatol. 1995;22:1281–5.
15. Steen VD, Powell DL, Medsger TAJ. Clinical correlations and prognosis based on serum autoantibodies in patients with systemic sclerosis. Arthritis Rheum. 1988;31:196–203.
16. Kuwana M, Sato S, Kikuchi K, Kawaguchi Y, Fujisaku A, Misaki Y, et al. Evaluation of functional disability using the health assessment questionnaire in Japanese patients with systemic sclerosis. J Rheumatol. 2003;30(6):1253–8.
17. Chen R, Lowe L, Wilson JD, Crowther E, Tzeggai K, Bishop JE, et al. Simultaneous quantification of six human cytokines in a single sample using microparticle-based flow cytometric technology. Clin Chem. 1999;45(9):1693–4.
18. Luster AD. Chemokines—chemotactic cytokines that mediate inflammation. N Eng J Med. 1998;338:436–45.
19. Lee EB, Zhao J, Kim JY, Xiong M, Song YW. Evidence of potential interaction of chemokine genes in susceptibility to systemic sclerosis. Arthritis Rheum. 2007;56(7):2443–8.
20. Furuse S, Fujii H, Kaburagi Y, Fujimoto M, Hasegawa M, Takehara K, et al. Serum concentrations of the CXC chemokines interleukin 8 and growth-regulated oncogene-alpha are elevated in patients with systemic sclerosis. J Rheumatol. 2003;30(7): 1524–8.
21. Codullo V, Baldwin HM, Singh MD, Fraser AR, Wilson C, Gilmour A, et al. An investigation of the inflammatory cytokine and chemokine network in systemic sclerosis. Ann Rheum Dis. 2011;70(6):1115–21.
22. Gourh P, Arnett FC, Assassi S, Tan FK, Huang M, Diekman L, et al. Plasma cytokine profiles in systemic sclerosis: associations with autoantibody subsets and clinical manifestations. Arthritis Res Ther. 2009;11(5):R147.
23. Koch AE, Kronfeld-Harrington LB, Szekanecz Z, Cho MM, Haines GK, Harlow LA, et al. In situ expression of cytokines and cellular adhesion molecules in the skin of patients with systemic sclerosis. Pathobiology. 1993;61:239–46.
24. Kadono T, Kikuchi K, Ihn H, Takehara K, Tamaki K. Increased production of interleukin 6 and interleukin 8 in scleroderma fibroblasts. J Rheumatol. 1998;25(2):296–301.
25. Keane MP, Arenberg DA, Lynch JP 3rd, Whyte RI, Iannettoni MD, Burdick MD, et al. The CXC chemokines, IL-8 and IP-10, regulate angiogenic activity in idiopathic pulmonary fibrosis. J Immunol. 1997;159(3):1437–43.
26. Bolster MB, Ludwicka A, Sutherland SE, Strange C, Silver RM. Cytokine concentrations in bronchoalveolar lavage fluid of patients with systemic sclerosis. Arthritis Rheum. 1997;40: 746–51.
27. Schmidt K, Martinez-Gamboa L, Meier S, Witt C, Meisel C, Hanitsch LG, et al. Bronchoalveoloar lavage fluid cytokines and chemokines as markers and predictors for the outcome of interstitial lung disease in systemic sclerosis patients. Arthritis Res Ther. 2009;11(4):R111.
28. Wolff B, Burns AR, Middleton J, Rot A. Endothelial cell "memory" of inflammatory stimulation: human venular endothelial cells store interleukin 8 in Weibel–Palade bodies. J Exp Med. 1998;188(9):1757–62.
29. Utgaard JO, Jahnsen FL, Bakka A, Brandtzaeg P, Haraldsen G. Rapid secretion of prestored interleukin 8 from Weibel–Palade bodies of microvascular endothelial cells. J Exp Med. 1998; 188(9):1751–6.

30. Distler O, Pap T, Kowal-Bielecka O, Meyringer R, Guiducci S, Landthaler M, et al. Overexpression of monocyte chemoattractant protein 1 in systemic sclerosis: role of platelet-derived growth factor and effects on monocyte chemotaxis and collagen synthesis. Arthritis Rheum. 2001;44(11):2665–78.
31. Gu L, Tseng S, Horner RM, Tam C, Loda M, Rollins BJ. Control of TH2 polarization by the chemokine monocyte chemoattractant protein-1. Nature. 2000;404(6776):407–11.
32. Distler JH, Jungel A, Caretto D, Schulze-Horsel U, Kowal-Bielecka O, Gay RE, et al. Monocyte chemoattractant protein 1 released from glycosaminoglycans mediates its profibrotic effects in systemic sclerosis via the release of interleukin-4 from T cells. Arthritis Rheum. 2006;54(1):214–25.
33. Gharaee-Kermani M, Denholm EM, Phan SH. Costimulation of fibroblast collagen and transforming growth factor beta1 gene expression by monocyte chemoattractant protein-1 via specific receptors. J Biol Chem. 1996;271(30):17779–84.
34. Carulli MT, Ong VH, Ponticos M, Shiwen X, Abraham DJ, Black CM, et al. Chemokine receptor CCR2 expression by systemic sclerosis fibroblasts: evidence for autocrine regulation of myofibroblast differentiation. Arthritis Rheum. 2005;52(12):3772–82.
35. Hasegawa M, Sato S, Takehara K. Augmented production of chemokines (monocyte chemotactic protein-1 (MCP-1), macrophage inflammatory protein-1alpha (MIP-1alpha) and MIP-1beta) in patients with systemic sclerosis: MCP-1 and MIP-1alpha may be involved in the development of pulmonary fibrosis. Clin Exp Immunol. 1999;117(1):159–65.
36. Antonelli A, Ferri C, Fallahi P, Ferrari SM, Giuggioli D, Colaci M, et al. CXCL10 (alpha) and CCL2 (beta) chemokines in systemic sclerosis—a longitudinal study. Rheumatology (Oxford). 2008;47(1):45–9.
37. Hasegawa M, Fujimoto M, Matsushita T, Hamaguchi Y, Takehara K, Sato S. Serum chemokine and cytokine levels as indicators of disease activity in patients with systemic sclerosis. Clin Rheumatol. 2011;30(2):231–7.
38. Kaplanski G, Marin V, Montero-Julian F, Mantovani A, Farnarier C. IL-6: a regulator of the transition from neutrophil to monocyte recruitment during inflammation. Trends Immunol. 2003;24(1):25–9.
39. Distler O, Rinkes B, Hohenleutner U, Scholmerich J, Landthaler M, Lang B, et al. Expression of RANTES in biopsies of skin and upper gastrointestinal tract from patients with systemic sclerosis. Rheumatol Int. 1999;19(1–2):39–46.
40. Anderegg U, Saalbach A, Haustein UF. Chemokine release from activated human dermal microvascular endothelial cells—implications for the pathophysiology of scleroderma? Arch Dermatol Res. 2000;292(7):341–7.
41. Scala E, Pallotta S, Frezzolini A, Abeni D, Barbieri C, Sampogna F, et al. Cytokine and chemokine levels in systemic sclerosis: relationship with cutaneous and internal organ involvement. Clin Exp Immunol. 2004;138(3):540–6.
42. Fujii H, Shimada Y, Hasegawa M, Takehara K, Sato S. Serum levels of a Th1 chemoattractant IP-10 and Th2 chemoattractants, TARC and MDC, are elevated in patients with systemic sclerosis. J Dermatol Sci. 2004;35(1):43–51.
43. Rabquer BJ, Tsou PS, Hou Y, Thirunavukkarasu E, Haines GK 3rd, Impens AJ, et al. Dysregulated expression of MIG/CXCL9, IP-10/CXCL10 and CXCL16 and their receptors in systemic sclerosis. Arthritis Res Ther. 2011;13(1):R18.

OPEN ACCESS Freely available online

PLOS ONE

Fli1 Represses Transcription of the Human α2(I) Collagen Gene by Recruitment of the HDAC1/p300 Complex

Yoshihide Asano[1]*, Maria Trojanowska[2]

1 Department of Dermatology, University of Tokyo Graduate School of Medicine, Tokyo, Japan, **2** Arthritis Center, Boston University School of Medicine, Boston, Massachusetts, United States of America

Abstract

Fli1, a member of the Ets transcription factor family, is a key repressor of the human α2(I) collagen (COL1A2) gene. Although our previous studies have delineated that TGF-β induces displacement of Fli1 from the COL1A2 promoter through sequential post-translational modifications, the detailed mechanism by which Fli1 functions as a potent transcriptional repressor of the COL1A2 gene has not been fully investigated. To address this issue, we carried out a series of experiments especially focusing on protein-protein interaction and epigenetic transcriptional regulation. The combination of tandem affinity purification and mass spectrometry identified HDAC1 as a Fli1 interacting protein. Under quiescent conditions, HDAC1 induced deacetylation of Fli1 resulting in an increase of Fli1 DNA binding ability and p300 enhanced this process by promoting the formation of a Fli1-HDAC1-p300 complex. TGF-β-induced phosphorylation of Fli1 at threonine 312 led to disassembly of this protein complex. In quiescent dermal fibroblasts Fli1, HDAC1, and p300 occupied the −404 to −237 region, including the Fli1 binding site, of the COL1A2 promoter. TGF-β induced Fli1 and HDAC1 dissociation from the COL1A2 promoter, while promoting Ets1 and p300 recruitment. Furthermore, acetylation levels of histone H3 around the Fli1 binding site in the COL1A2 promoter inversely correlated with the DNA occupancy of Fli1 and HDAC1, while positively correlating with that of Ets1 and p300. In the functional studies, HDAC1 overexpression magnified the inhibitory effect of Fli1 on the COL1A2 promoter. Moreover, pharmacological blockade of HDAC1 by entinostat enhanced collagen production in dermal fibroblasts. Collectively, these results indicate that under quiescent conditions Fli1 recruits HDAC1/p300 to the COL1A2 promoter and suppresses the expression of the COL1A2 gene by chromatin remodeling through histone deacetylation. TGF-β-dependent phosphorylation of Fli1 at threonine 312 is a critical step regulating the remodeling of the Fli1 transcription repressor complex, leading to transcriptional activation of the COL1A2 gene.

Citation: Asano Y, Trojanowska M (2013) Fli1 Represses Transcription of the Human α2(I) Collagen Gene by Recruitment of the HDAC1/p300 Complex. PLoS ONE 8(9): e74930. doi:10.1371/journal.pone.0074930

Editor: Nicoletta Landsberger, University of Insubria, Italy

Received May 1, 2013; **Accepted** August 7, 2013; **Published** September 13, 2013

Funding: This study was supported by the NIH grant AR42334. The funders had no role in study design, data collection and analysis, decision to publish, or preparation of the manuscript.

Competing Interests: The authors have declared that no competing interests exist.

* E-mail: yasano-tky@umin.ac.jp

Introduction

Fli1 is a member of the Ets transcription factor family that was initially identified as a proto-oncogene in Friend virus-induced erythroleukemia in mice [1,2]. In humans, Fli1 is frequently involved in the development of Ewing sarcoma and related subtypes of primitive neuroectodermal tumors [3], suggesting that Fli1 plays an important role in the process of cellular transformation. In normal tissues, Fli1 is preferentially expressed in endothelial and hematopoietic cell lineages [4] and participates in the regulation of the development and differentiation of these cell types. Extensive *in vitro* studies as well as the data obtained from various Fli1 mutant mice support a crucial role of Fli1 in megakaryocytic differentiation and myelomonocytic, erythroid, and NK cell development [5–8]. Furthermore, Fli1 knockout mice die during embryogenesis with a loss of vascular integrity leading to cerebral hemorrhage, suggesting that Fli1 is involved in the regulation of genes critical for vascular remodeling [5]. Endothelial Fli1 deficiency affects vascular homeostasis through the impairment of endothelial adhesion junctions, vascular basement membrane remodeling, and endothelial cell-pericyte interactions as described in our previous report [9].

Although Fli1 is present in a relatively limited amount in dermal fibroblasts, Fli1 plays a pivotal role in the regulation of the extracellular matrix (ECM) and its related molecules, including type I collagen [10–12], tenascin-C [13,14], ECM-degrading enzymes [15–17] and the multifunctional matricellular factor CCN2 [18]. Most importantly, Fli1 has been shown to be a potent inhibitor of type I collagen production in dermal fibroblasts and persistent downregulation of this transcription factor has been implicated in the pathogenesis of cutaneous fibrosis in scleroderma [12,19]. The data from our laboratory and others demonstrated that Fli1 binds to the human α2(I) collagen (COL1A2) promoter under physiological conditions, but dissociates from the promoter in response to TGF-β stimulation [10,11]. Given that gene silencing of Fli1 results in a robust increase of type I collagen production [18], this process is critical for the TGF-β-dependent up-regulation of the type I collagen gene. Our recent studies have elucidated the principal mechanism responsible for TGF-β-dependent regulation of Fli1 activity in the context of the COL1A2 promoter [20–22]. This pathway is initiated by TGF-β-dependent activation of c-Abl tyrosine kinase that mediates nuclear translocation of protein kinase C-δ (PKC-δ) and phosphorylation of Fli1 at threonine 312. This modification

triggers subsequent Fli1 acetylation at lysine 380 by p300/CREB-binding protein-associated factor (PCAF) and displacement of Fli1 from the COL1A2 promoter. However, the mechanism through which Fli1 exerts its potent inhibitory effect on COL1A2 gene expression has not yet been elucidated.

Earlier studies from our laboratory and others have suggested that Fli1 and Ets1 compete for the binding of the Ets binding domain in the COL1A2 promoter and the ratio of Ets1/Fli1 plays an important role in the regulation of promoter activity [10]. However, our earlier study also demonstrated that the Fli1 W321R mutant, which does not bind to DNA, as well as a deletion construct containing only the Ets domain exert a more modest but consistently reproducible inhibitory effect on COL1A2 promoter activity compared with wild type Fli1, suggesting that an indirect mechanism as well as a direct mechanism contribute to the inhibitory effects of Fli1 on the COL1A2 promoter activity. The purpose of this study was to further investigate the molecular mechanism by which Fli1 exerts its inhibitory effect on COL1A2 gene. By a series of experiments, we demonstrated that Fli1 recruits HDAC1 to the COL1A2 promoter and decreases the acetylation levels of histone H3. These results indicate that Fli1 functions as a potent transcriptional repressor through chromatin modification as well as competition with transcriptional activator Ets1.

Materials and Methods

Ethics Statement

Human dermal fibroblast cultures were established from the foreskins of healthy newborns from the Medical University of South Carolina Hospital. This study was approved by the Medical University of South Carolina Institutional Review Board for Human Research, and written informed consent was obtained from both parents of the child. The whole study was performed according to the Declaration of Helsinki.

Reagents

Recombinant human TGF-β1 was obtained from PeproTech (Rocky Hill, NJ, USA). The polyclonal rabbit anti-Fli1 antibody was described previously [8]. The monoclonal mouse anti-Fli1 antibody was purchased from BD Bioscience (Bedford, MA, USA). The polyclonal rabbit anti-acetylated lysine antibodies, anti-HA tag antibody and anti-HDAC1 antibody were purchased from Cell Signaling Technology (Danvers, MA, USA). Antibodies for β-actin and Flag tag were purchased from Sigma-Aldrich (St. Louis, MO, USA). Antibodies for p300, PCAF, and Ets1 were obtained from Santa Cruz Biotechnology (Santa Cruz, CA, USA). The antibody for calmodulin binding peptide was purchased from Millipore (Billerica, MA, USA). Entinostat was purchased from Selleck Chemicals (Houston, TX, USA). Adenoviral vectors expressing Fli1, green fluorescence protein, Fli1 siRNA or scrambled non-silencing RNA were generated as described previously [12,23].

Cell Cultures

Human dermal fibroblast cultures were established from the foreskins of healthy newborns from the Medical University of South Carolina Hospital as described previously [21]. All studies used cells from passage number 3 to 6. Before stimulation with TGF-β or entinostat, fibroblasts were incubated in serum-free medium for 48 hours. Human embryonic kidney 293T cells were purchased from ATCC and maintained in DMEM supplemented with 10% fetal bovine serum.

Plasmid Construction

pSG5-Fli1 and pCTAP-Fli1, which has two different tags, including a streptavidin binding peptide (SBP) and a calmodulin binding peptide, were described previously [20]. A -772 COL1A2/CAT construct was generated as previously described [5]. The expression vector of p300 was a gift from Dr Boyes (Institute of Cancer Research, London, UK). Expression vectors of PCAF and PCAF/ΔHAT, which lacks histone acetyltransferase (HAT) activity, were gifts from Dr Kouzarides (Cambridge University, Cambridge, UK). Plasmids were purified twice on cesium chloride gradients. At least two different plasmid preparations were used for each experiment.

Protein Isolation by Tandem Affinity Purification and Mass Spectrometry

The InterPlay Mammalian TAP System (Stratagene, La Jolla, CA, USA) was employed according to the manufacturer's instructions. The cDNA encoding human the Fli1 gene and two tandem affinity tags derived from the pCTAP-Fli1 vector was cloned into adenoviral shuttle vectors and linearized for *in vitro* ligation with the adenoviral backbone construct lacking the E1, E3, and E4 regions of the adenovirus genome. The pCTAP-Fli1 adenovirus expresses green fluorescence protein and tagged Fli1 under the control of two separate cytomegalovirus promoter/enhancers. Human dermal fibroblasts (1×10^8) were transduced with the pCTAP-Fli1 adenovirus. After 72 hours, cells were harvested and resuspended in lysis buffer supplemented with protease inhibitors. Cells underwent three rounds of freeze-thawing, cell debris was pelleted by centrifugation at 16,000×g for 10 minutes, and the supernatant was collected. Next, EDTA (2 mM final concentration), β-mercaptoethanol (10 mM final concentration), and streptavidin resin were added to the cell lysate and incubated at 4°C for 2 hours. The resin was collected by centrifugation at 1,500×g for 5 minutes, washed twice, and incubated in streptavidin elution buffer for 30 minutes at 4°C. To further purify the protein complexes, calmodulin resin and calmodulin binding buffer were added to the supernatant. After 2-hour incubation at 4°C, the resin was collected (centrifugation at 1,500×g for 5 minutes) and washed twice. Then, protein complexes were eluted by adding calmodulin elution buffer and incubation for 30 minutes at 4°C. The resulting eluate was concentrated by trichloroacetic precipitation, resolved by two-dimensional gel electrophoresis, and visualized on the gel by silver staining. In a control experiment, the pull-down approach was performed with beads only. Bands which appeared on the gel from the Fli1 overexpression experiment but not the control experiment were excised and sent for mass spectrometry analysis to the Mass Spectrometry Facility at Medical University of South Carolina. According to the quality requirements of the facility, a protein can only be considered as an interactor if two or more peptides match the respective protein in the Swiss-Prot database.

Immunoblotting

Whole cell extracts were prepared using lysis buffer with the following contents: 1% Triton X-100, 50 mM Tris-HCl [pH 7.4], 150 mM NaCl, 3 mM $MgCl_2$, 1 mM $CaCl_2$, proteinase inhibitor cocktail (Roche Applied Sciences, Indianapolis, IN, USA), 1 mM phenylmethyl sulfonyl fluoride and 100 ng/ml of Trichostatin A (Sigma-Aldrich). Protein extracts were subjected to SDS-PAGE and transferred to nitrocellulose membranes. Membranes were incubated overnight with primary antibody, washed, and incubated for 1 hour with secondary antibody. After washing,

visualization was performed by enhanced chemiluminescence (Pierce, Rockford, IL, USA).

Immunoprecipitation

To precipitate non-tagged proteins, whole cell extracts (500 μg) were pre-adsorbed with protein G sepharose beads (GE Healthcare, Waukesha, WI, USA) and incubated with 2 μg of appropriate antibodies and then with protein G sepharose beads. Streptavidin-coupled agarose beads (Sigma-Aldrich) were used instead of protein G sepharose beads for immunoprecipitation of ectopically expressed tagged-Fli1. The precipitated proteins were subjected to immunoblotting.

In vivo Acetylation Assay

293 T cells were transfected with expression vectors encoding tagged-Fli1 (0.1 μg) and the indicated HAT protein (2 μg), and incubated for 48 hours. Whole cell lysates (500 μg) were incubated with 10 μl of streptavidin-coupled agarose beads overnight at 4°C. Precipitated proteins were subjected to immunoblotting using a rabbit anti-acetylated lysine antibody. After development, the membrane was stripped and reprobed with an anti-calmodulin binding peptide antibody to determine the total levels of ectopically expressed Fli1.

DNA Affinity Precipitation Assay

DNA affinity precipitation (DNAP) was carried out as described previously [21]. Briefly, whole cell extracts (500 μg) prepared from 293 T cells were incubated for 10 minutes at 4°C with gel shift binding buffer (10 mM Tris-HCl [pH 8.0], 40 mM KCl, 1 mM DTT, 6% glycerol, 0.05% NP-40), and 20 μg of poly(dI-dC) (Pierce) in a final volume of 1 ml. Preclearing was performed by adding streptavidin-coupled agarose beads and incubating the mixture for 30 minutes with gentle rocking at 4°C. After centrifugation, the supernatant was incubated with 500 pmol of the COL1A2 Ets binding site (EBS) oligonucleotide overnight at 4°C with gentle rocking. Then, 65 μl of streptavidin-coated agarose beads was added, followed by a further 2-hour incubation at 4°C. The protein-DNA-streptavidin-agarose complex was washed twice with Tris-EDTA (100 mM NaCl), twice with gel shift binding buffer, and once with phosphate-buffered saline. The precipitates were subjected to immunoblotting using the anti-Fli1 antibody. The specific binding of Fli1 to the COL1A2 EBS oligonucleotide through EBS was demonstrated previously [11,20].

Chromatin Immunoprecipitation Assay

The chromatin immunoprecipitation (ChIP) assay was carried out essentially as described previously [18]. Briefly, cells were treated with 1% formaldehyde for 10 minutes. The cross-linked chromatin was then prepared and sonicated to an average size of 300–500 bp. The DNA fragments were immunoprecipitated overnight with or without polyclonal anti-Fli1 antibody at 4°C. After reversal of cross-linking, the immunoprecipitated chromatin was amplified by PCR amplification of specific regions of the COL1A2 genomic locus. The primers were as follows: COL1A2/F-404:5′-CTGGACAGCTCCTGCTTTGAT-3′, COL1A2/R-233; 5′-CTTTCAAGGGGAAACTCTGACTC-3′. The amplified DNA products were resolved by agarose gel electrophoresis.

Reverse Transcription Quantitative Real-time PCR

Total RNA was isolated from confluent fibroblasts using Tri reagent (MRC Inc., Cincinnati, OH, USA) according to the manufacturer's instructions. Two μg of RNA was used for reverse transcription cDNA synthesis in a 20 μl reaction volume using random primers and then diluted to 40 μl. Quantitative real-time PCR was carried out using IQ Sybr green mix and an Icycler machine (BIO-RAD, Hercules, CA, USA) using 1 μl of diluted cDNA in triplicate with β-actin as the internal control. PCR conditions were 95°C for 3 minutes, followed by 40 cycles of 95°C for 30 seconds, 58°C for 1 minute. Melt curve analysis of the PCR products confirmed the absence of secondary products. The sequences of α1(I) collagen and β-actin primers were previously reported [18].

Statistical Analysis

Data presented as bar graphs are the means ± SD of at least three independent experiments. Statistical analysis was performed using the Mann Whitney-U test ($p<0.05$ was considered significant).

Results

HDAC1 Interacts with Fli1 and Mediates its Deacetylation

As an initial experiment, we employed a proteomic analysis to identify nuclear factors that form a complex with Fli1 in dermal fibroblasts. To this end, adenovirus expressing Fli1 with two tags (Figure 1A) was transduced into dermal fibroblasts and the transcription factor complex including Fli1 was purified according to the manufacturer's instructions. Purified protein complex was subjected to two-dimensional gel electrophoresis and several spots were identified in the gel stained with silver (data not shown). Proteins were extracted from each spot and subjected to mass spectrometry. One of the most consistently identified proteins was histone deacetylase 1 (HDAC1). To further confirm interaction of Fli1 with HDAC1 under physiological conditions, immunoprecipitation was performed using cell lysates prepared from quiescent dermal fibroblasts. As shown in Figure 1B, Fli1 formed a complex with HDAC1, but not with HDAC3. We next investigated if HDAC1 regulates acetylation levels of Fli1 by an *in vivo* acetylation assay using 293 T cells. Since PCAF mediates Fli1 acetylation, we examined the effect of forced expression of HDAC1 on acetylation levels of Fli1 in the presence of either PCAF or PCAF/ΔHAT. Expectedly, forced expression of HDAC1 markedly decreased the basal and PCAF-dependent acetylation of Fli1 (Figure 1C). To further confirm the involvement of HDAC1 in the regulation of Fli1 acetylation, we employed a gene-silencing technique using an antisense oligonucleotide. A pilot experiment established that the HDAC1 antisense oligonucleotide, which was previously shown to efficiently suppress the levels of HDAC1 protein [24], was superior in decreasing expression levels of HDAC1 in comparison with commercially available HDAC1 siRNA (data not shown). As shown in Figure 1D, the suppression of HDAC1 expression by the antisense oligonucleotide led to an increase of acetylation levels of Fli1, especially in the presence of PCAF. Taken together, these results indicate that HDAC1 interacts with Fli1 and subsequently mediates its deacetylation.

p300 Promotes the Interaction of Fli1 with HDAC1 and Increases the DNA Binding Ability of Fli1 through Deacetylation of Lysine 380

Our previous studies have shown that PCAF-dependent acetylation of Fli1 at lysine 380 decreases its protein stability [20]. In the course of these experiments, we also noticed that p300 increases the protein stability of Fli1 (unpublished data). Given that acetylation of Fli1 decreases its protein stability [20], this observation suggested that p300 might influence Fli1 acetylation.

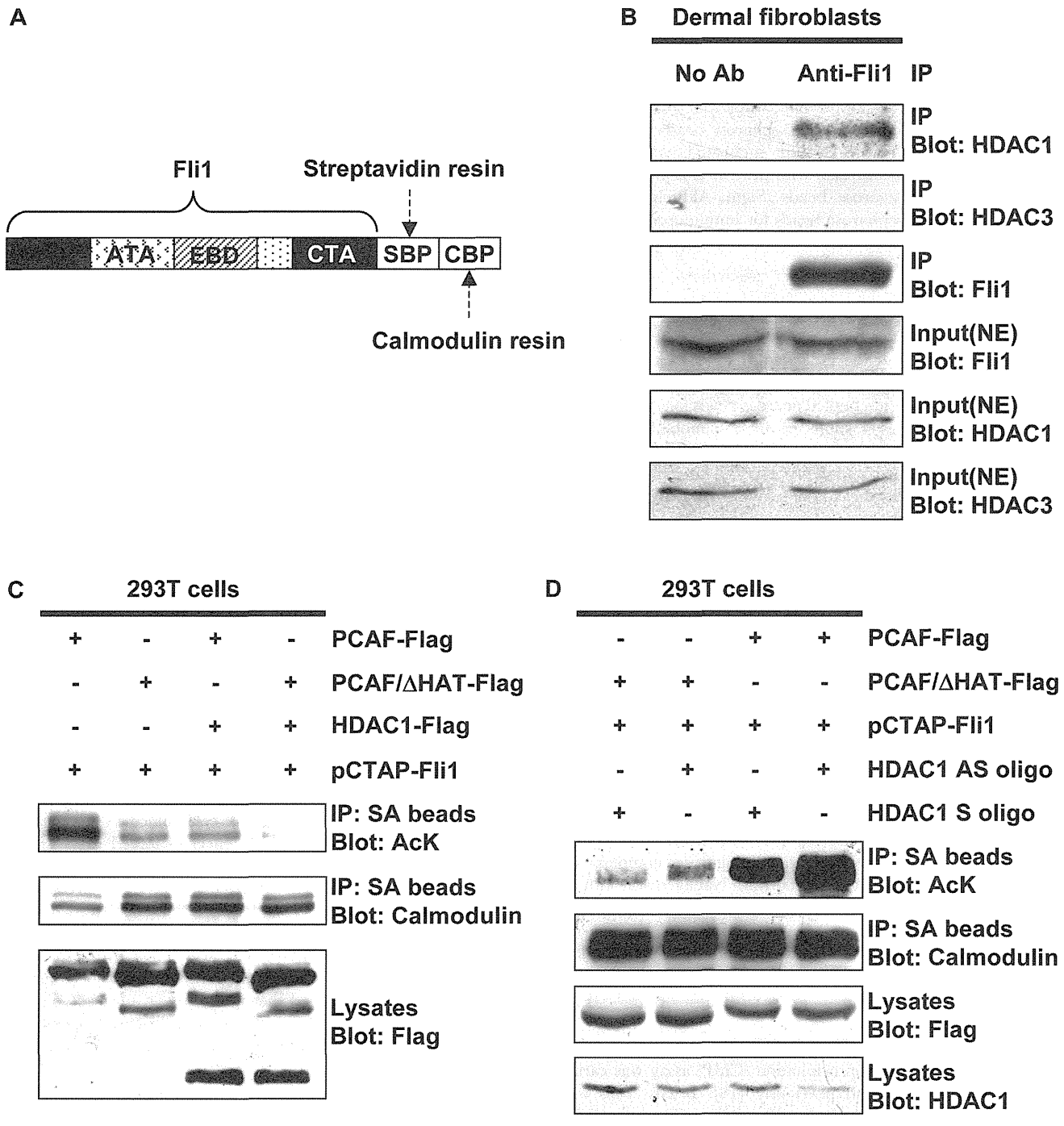

Figure 1. HDAC1 interacts with Fli1 and mediates its deacetylation. A. A schematic representation of pCTAP-Fli1. Streptavidin and calmodulin resins bind to streptavidin-binding peptide (SBP) and calmodulin-binding peptide (CBP), respectively. ATA: A-terminal activation domain, EBD: Ets binding domain, CTA: C-terminal activation domain. **B.** Foreskin fibroblasts were grown to subconfluence and serum-starved for 48 hours. Equal amount of protein from whole cell lysates was subjected to immunoprecipitation with or without anti-Fli1 antibody. The levels of Fli1, HDAC1, and HDAC3 proteins in precipitates were determined by immunoblotting. The levels of Fli1, HDAC1 and HDAC3 in whole cell lysates were determined by Western blotting. **C.** 293 T cells were transfected with pCTAP expression vector encoding wild type Fli1 along with PCAF, PCAFΔHAT, or HDAC1 expression vectors, and incubated for 48 hours. Total cell extracts were subjected to immunoprecipitation using streptavidin-coupled agarose beads (SA beads), followed by immunoblotting using rabbit anti-acetylated lysine antibody (AcK). To visualize the total levels of ectopically expressed Fli1, the same membrane was stripped and reprobed with anti-calmodulin binding peptide antibody. The levels of Flag-tagged proteins in cell lysates were determined by Western blotting. **D.** 293 T cells were transfected with pCTAP wild type Fli1 along with PCAF or PCAFΔHAT expression vectors. Six hours after the transfection, HDAC1 antisense oligonucleotide (HDAC1 AS oligo) or HDAC1 sense oligonucleotide (HDAC1 S oligo) were added to the cells. Whole cells lysates were prepared 48 hours after transfection. The levels of acetylated Fli1 and Flag-tagged proteins were determined as described above. The efficacy of HDAC1 AS oligo was evaluated by Western blotting.
doi:10.1371/journal.pone.0074930.g001

To address this point, we carried out an *in vivo* acetylation assay using 293 T cells. As shown in Figure 2A, consistent with our previous report, forced expression of PCAF resulted in a robust increase of Fli1 acetylation. In contrast, low acetylation levels of Fli1 were observed in the presence of either p300 or p300/ΔHAT, suggesting that HAT activity of p300 does not acetylate Fli1. Importantly, PCAF-induced acetylation levels of Fli1 were decreased in the presence of p300, suggesting that p300 interferes with Fli1 acetylation by PCAF. Since acetylation reduces the DNA binding ability of Fli1 [20], we utilized DNAP to investigate the effect of p300 on the DNA binding ability of Fli1. As shown in Figure 2B, in contrast to PCAF, p300 increased DNA binding ability of Fli1. Furthermore, co-expression of p300 reversed the PCAF-dependent decrease of DNA binding of Fli1. To further investigate if p300 increases the DNA binding ability of Fli1 through deacetylation, we performed DNAP using a mutant of Fli1 (K380Q) that mimics the constitutively acetylated form of Fli1. As shown in Figure 2C, DNA binding of Fli1 K380Q mutant was markedly decreased compared with wild type Fli1, indicating that this mutant has the same property as the constitutively acetylated form of Fli1. In contrast to wild type Fli1, forced expression of p300 did not affect the DNA binding ability of Fli1 K380Q mutant, suggesting that p300 promotes the DNA binding of Fli1 by modulating acetylation status of Fli1. Given that p300 promoted deacetylation of Fli1 despite lacking histone deacetylase activity, it was speculated that p300 potentially enhances the interaction between Fli1 and HDAC1, leading to Fli1 deacetylation, or alternatively that p300 prevents Fli1 acetylation by competing for its interaction with PCAF. To address this point, we investigated the interaction of Fli1 with HDAC1 in the presence or absence of p300. Since 293T cells have a relatively low amount of HAT proteins, we employed this cell line for the experiment. As shown in Figure 2D, in the absence of p300, the interaction of Fli1 with HDAC1 was marginal. In contrast, forced expression of p300 resulted in increased interaction of Fli1 with HDAC1. On the other hand, in 293T cells transfected with Fli1 and PCAF, co-expression of p300 did not affect the interaction of Fli1 with PCAF (data not shown). Collectively, these results indicate that p300 promotes deacetylation of Fli1 by facilitating interaction of Fli1 with HDAC1, consistent with the increased DNA binding of Fli1.

Phosphorylation of Fli1 at Threonine 312 Decreases its Interactions with p300 and HDAC1

Previous studies have shown that phosphorylation of Fli1 at threonine 312 is required for its subsequent interaction with PCAF and acetylation at lysine 380 [21]. Since, as shown here, this process is also modulated by p300, we asked whether the Fli1 phosphorylation status affects its interaction with p300. To address this point, we compared complex formation of wild type Fli1 and a phosphorylation resistant mutant of Fli1 (Fli1 T312A) with p300 in 293T cells. As shown in Figure 3A, interaction with p300 was remarkably increased in the Fli1 T312A mutant compared with wild type Fli1, suggesting that the unphosphorylated form of Fli1 preferably forms a complex with p300. Next, we investigated whether Fli1 modulates the interaction of p300 with HDAC1. As shown in Figure 3B, p300 formed a complex with HDAC1. Importantly, forced expression of Fli1 increased this interaction (left panels), whereas gene silencing of Fli1 decreased the interaction of p300 with HDAC1 (right panels). Taken together, these results suggest that the unphosphorylated form of Fli1 recruits p300 and HDAC1 to form the transcription repressor complex. This notion was further confirmed under physiological conditions (Figure 3C). Since the peak of Fli1 phosphorylation occurs at 2 hours after TGF-β stimulation, we examined this time point. As predicted, association of Fli1 with p300 and HDAC1 was decreased at 2 hours after addition of TGF-β. Collectively, these results suggest that TGF-β-dependent phosphorylation of Fli1 at threonine 312 is a critical event regulating the remodeling of the Fli1 repressor complex.

TGF-β-induced Histone H3 Acetylation Correlates with Fli1/HDAC1 Dissociation and Ets1/p300 Recruitment in the Context of the COL1A2 Promoter

Based on the current data described above, we hypothesized that Fli1 recruits HDAC1 to the COL1A2 promoter and promotes histone deacetylation and subsequent chromatin condensation, resulting in the suppression of COL1A2 gene expression. To assess this hypothesis, we first investigated the status of histone H3 acetylation around the Ets binding site in the COL1A2 promoter. As shown in Figure 4A, the acetylated form of histone H3 (Ac-H3) was detectable in this promoter region of unstimualted cells. Upon treatment with histone deacetylase inhibitor, Trichostatin A, the level of Ac-H3 increased, while after treatment with Anacardic acid, an inhibitor of HAT proteins, the level of Ac-H3 decreased, suggesting that this promoter region is subject to an active chromatin remodeling. Next, we examined the effect of TGF-β on the DNA occupancy of Fli1, Ets1, p300, and HDAC1 and on the level of Ac-H3 in the COL1A2 promoter. Consistent with our previous results, Fli1 occupied the COL1A2 promoter in unstimulated cells. Furthermore, in agreement with the *in vitro* findings HDAC1 was also present in this promoter region. However, there were only low levels of bound Ets1, p300, and Ac-H3 (Figure 4B). After 3 hours of TGF-β treatment DNA binding of Fli1 and HDAC1 was decreased, while DNA binding of Ets1 and p300 and the level of Ac-H3 were markedly increased. These results illustrate a dynamic remodeling of transcription factor complex on the COL1A2 promoter *in vivo* in response to TGF-β.

HDAC1 Inhibits Collagen Gene Expression in Dermal Fibroblasts

To determine whether manipulation of HDAC1 has an effect on collagen gene expression, we investigated the impact of HDAC1 on the COL1A2 promoter activity. To this end, we employed a CAT reporter analysis using the −772 COL1A2/CAT construct. As shown in Figure 5A, overexpression of Fli1 suppressed the basal activity of the −772 COL1A2/CAT promoter. Expectedly, coexpression of HDAC1 with Fli1 further suppressed the promoter activity of the −772 COL1A2/CAT construct in a dose-dependent manner. These results suggest that HDAC1 magnifies the inhibitory effect of Fli1 on the promoter activity of the COL1A2 gene through an increase of DNA binding of Fli1 as well as histone deacetylation. To further confirm if chromatin remodeling is involved in the mechanism responsible for Fli1-dependent suppression of COL1A2 promoter activity, we used the Fli1 K380R mutant, in which lysine 380 is replaced with arginine. Since Fli1 is acetylated by PCAF at lysine 380, this construct is resistant to PCAF-dependent acetylation and its DNA binding ability to COL1A2 promoter is markedly increased. Consistent with our previous data [20], Fli1 K380R suppressed the basal promoter activity of the COL1A2 gene to a much greater extent than wild type Fli1. When HDAC1 was co-expressed, the inhibitory effect of Fli1 K380R was further magnified. Given that HDAC1 co-expression did not affect the DNA binding of the Fli1 K380R construct (data not shown), these results indicate that HDAC1 further strengthens the inhibitory effect of Fli1 on the promoter activity of COL1A2 gene through histone deacetylation.

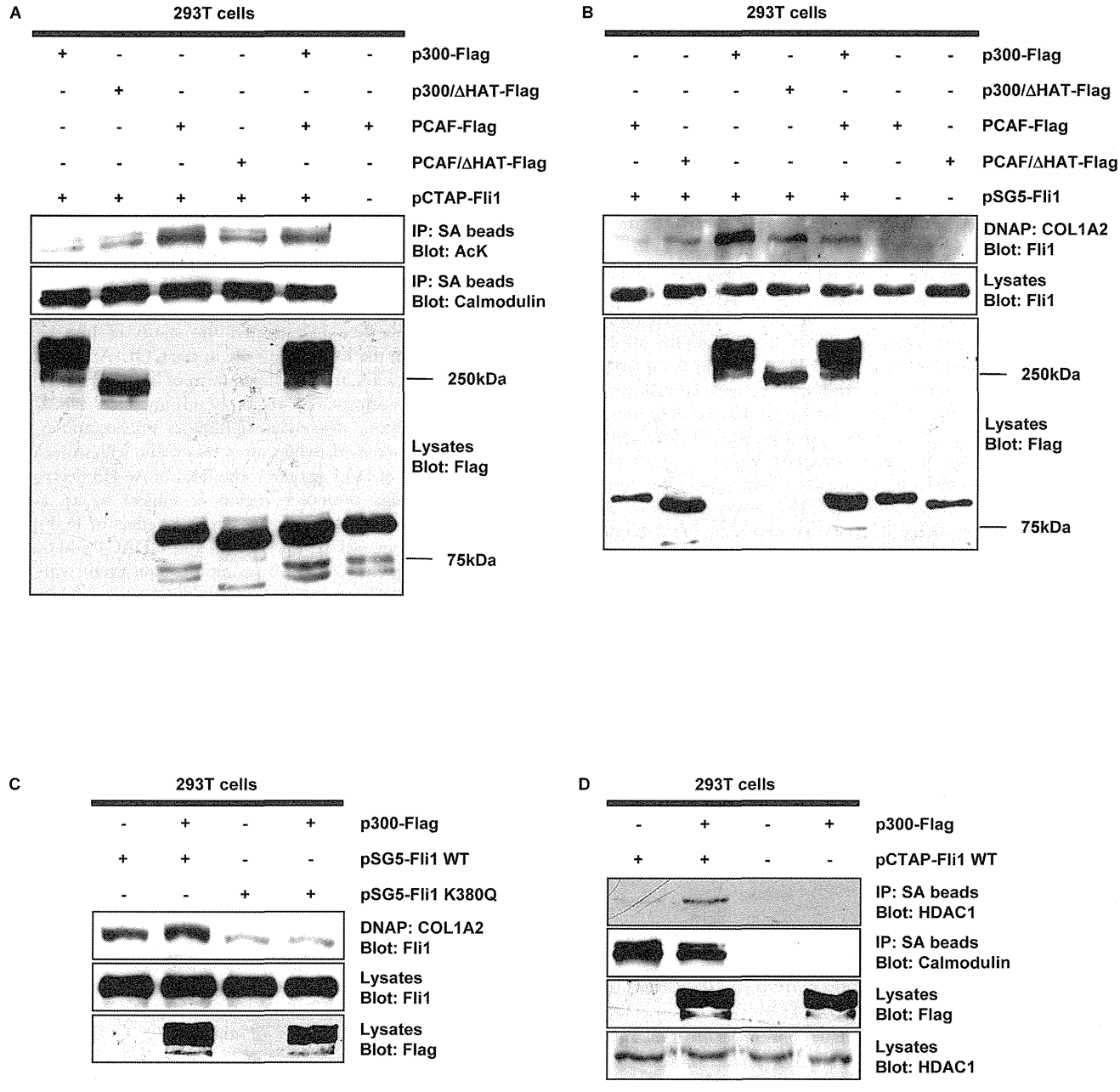

Figure 2. p300 increases the DNA binding ability of Fli1 through HDAC1-dependent deacetylation of lysine 380. A. 293T cells were transfected with pCTAP wild type Fli1 along with the indicated HAT proteins, and incubated for 48 hours. Total cell extracts were subjected to immunoprecipitation using streptavidin-coupled agarose beads (SA beads), followed by immunoblotting using rabbit anti-acetylated lysine antibody (AcK). In order to visualize the total levels of ectopically expressed Fli1, the same membrane was stripped and reprobed with anti-calmodulin binding peptide antibody. The levels of HAT proteins in cell lysates were determined by Western blotting. **B.** Whole cell lysates prepared as described above were incubated with biotin-labeled oligonucleotides. Proteins bound to these nucleotides were isolated with streptavidin-coupled agarose beads. The levels of Flag-tagged proteins and Fli1 in cell lysates were determined by Western blotting. **C.** 293T cells were transfected with pSG5 wild type Fli1 or Fli1 K380Q mutant along with the p300 expression vector, and incubated for 48 hours. **D.** 293T cells were transfected with pCTAP wild type Fli1 along with the p300 expression vector, and incubated for 48 hours. Total cell extracts were subjected to immunoprecipitation using SA beads, followed by immunoblotting using anti-HDAC1 antibody. To visualize the total levels of ectopically expressed Fli1, the same membrane was stripped and reprobed with anti-calmodulin binding peptide antibody. The levels of ectopically expressed p300 and endogenous HDAC1 in cell lysates were determined by Western blotting with anti-Flag antibody and anti-HDAC1 antibody, respectively.
doi:10.1371/journal.pone.0074930.g002

To evaluate the effect of the inhibition of HDAC1 on type I collagen gene expression, we utilized the specific pharmacological inhibitor of HDAC1, entinostat. Human dermal fibroblasts were treated with 1 μM entinostat for 48 hours and type I collagen expression was examined by immunoblotting and reverse transcription quantitative real-time PCR. As shown in Figure 5B and 5C, blockade of HDAC1 by entinostat significantly increased mRNA and protein levels of the type I collagen gene. Collectively, these results indicate that HDAC1 largely contributes to the regulation of type I collagen gene expression through chromatin

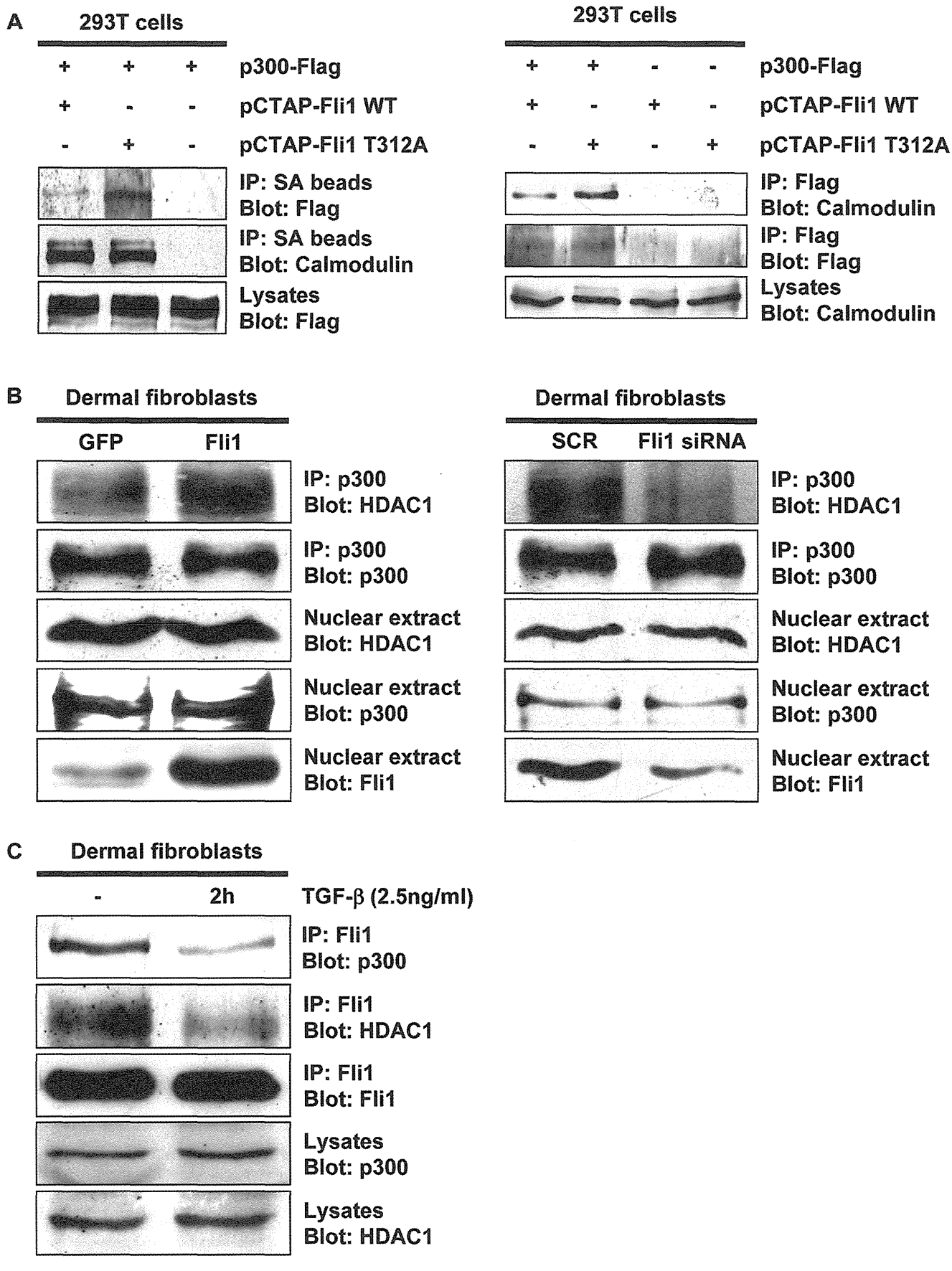
A
293T cells
+ + + p300-Flag
+ - - pCTAP-Fli1 WT
- + - pCTAP-Fli1 T312A
IP: SA beads
Blot: Flag
IP: SA beads
Blot: Calmodulin
Lysates
Blot: Flag
293T cells
+ + - - p300-Flag
+ - + - pCTAP-Fli1 WT
- + - + pCTAP-Fli1 T312A
IP: Flag
Blot: Calmodulin
IP: Flag
Blot: Flag
Lysates
Blot: Calmodulin
B
Dermal fibroblasts
GFP Fli1
IP: p300
Blot: HDAC1
IP: p300
Blot: p300
Nuclear extract
Blot: HDAC1
Nuclear extract
Blot: p300
Nuclear extract
Blot: Fli1
Dermal fibroblasts
SCR Fli1 siRNA
IP: p300
Blot: HDAC1
IP: p300
Blot: p300
Nuclear extract
Blot: HDAC1
Nuclear extract
Blot: p300
Nuclear extract
Blot: Fli1
C
Dermal fibroblasts
- 2h TGF-β (2.5ng/ml)
IP: Fli1
Blot: p300
IP: Fli1
Blot: HDAC1
IP: Fli1
Blot: Fli1
Lysates
Blot: p300
Lysates
Blot: HDAC1

Figure 3. Phosphorylation of Fli1 at threonine 312 decreases its interactions with p300 and HDAC1. A. 293T cells were transfected with pCTAP wild type Fli1 or the Fli1 T312A mutant along with the p300 expression vector, and incubated for 48 hours. Total cell extracts were subjected to immunoprecipitation using streptavidin-coupled agarose beads (SA beads) followed by immunoblotting with anti-Flag antibody (left panels), or to immunoprecipitation using the anti-Flag antibody followed by immunoblotting with anti-calmodulin antibody (right panels). The levels of ectopically expressed p300 or Fli1 in cell lysates were determined by Western blotting with anti-Flag antibody (the bottom left panel) or anti-calmodulin antibody (the bottom right panel), respectively. **B.** Foreskin fibroblasts were transduced with 25 MOI of Fli1 or green fluorescence protein (GFP) adenovirus for 72 hours (left panels), or/and 25 MOI of Fli1siRNA or scrambled RNA (SCR) adenovirus for 72 hours (right panels). Nuclear extracts were subjected to immunoprecipitation with anti-p300 antibody, followed by immunoblotting with anti-HDAC1 antibody. The levels of Fli1, p300, and HDAC1 in nuclear extracts were evaluated by Western blotting. **C.** Whole cell lysates prepared from untreated or TGF-β stimulated foreskin fibroblasts were subjected to immunoprecipitation with anti-Fli1 antibody, followed by immunoblotting with antibodies against p300, HDAC1, or Fli1. The levels of endogenous p300 and HDAC1 were examined by Western blotting.
doi:10.1371/journal.pone.0074930.g003

remodeling as a repressor complex "Fli1-p300-HDAC1" in human dermal fibroblasts.

Discussion

This study was undertaken to clarify the molecular mechanism by which Fli1 functions as a potent transcriptional repressor of the COL1A2 gene. We initially identified HDAC1 as a Fli1 interacting protein by combining tandem affinity purification and mass spectrometry. A series of experiments using an overexpression system in 293T cells demonstrated the following key findings: (i) the acetylation status of Fli1 is regulated by the balance between PCAF and HDAC1, (ii) p300 enhances the interaction between Fli1 and HDAC1 and Fli1 is maintained as a deacetylated form in the Fli1-HDAC1-p300 complex, resulting in an increase of its DNA binding ability, (iii) the unphosphorylated form of Fli1 preferably interacts with HDAC1 and p300. Given that TGF-β-dependent phosphorylation of Fli1 at threonine 312 promotes its interaction with PCAF and subsequently results in the loss of its DNA binding ability due to PCAF-dependent acetylation at lysine 380, it was speculated that TGF-β stimulation regulates the remodeling of the Fli1-HDAC1-p300 repressor complex through Fli1 phosphorylation at threonine 312. Supporting this idea, TGF-β decreased the interaction of Fli1 with HDAC1 and p300 in dermal fibroblasts at 2 hours after stimulation, when Fli1 phosphorylation at threonine 312 occurs. In ChIP analysis, more importantly, strong DNA binding of Fli1 and HDAC1 correlated with low levels of Ac-H3 in unstimualted dermal fibroblasts, while TGF-β-induced dissociation of Fli1 and HDAC1 and recruitment of Ets1 and p300 correlated with high levels of Ac-H3 (Figure 6). Given that forced expression of HDAC1 augmented the inhibitory effect of the Fli1 K380R mutant, whose DNA binding is not affected by HDAC1, on the COL1A2 promoter activity, Fli1 exerts its transcriptional repressor effect through HDAC1-dependent chromatin remodeling. Collectively, the current data clearly showed that Fli1 functions as a transcriptional repressor by promoting chromatin condensation due to HDAC1-dependent histone deacetylation and that phosphorylation of Fli1 at threonine 312 is a key post-translational modification regulating its association with HDAC1/p300 or with PCAF.

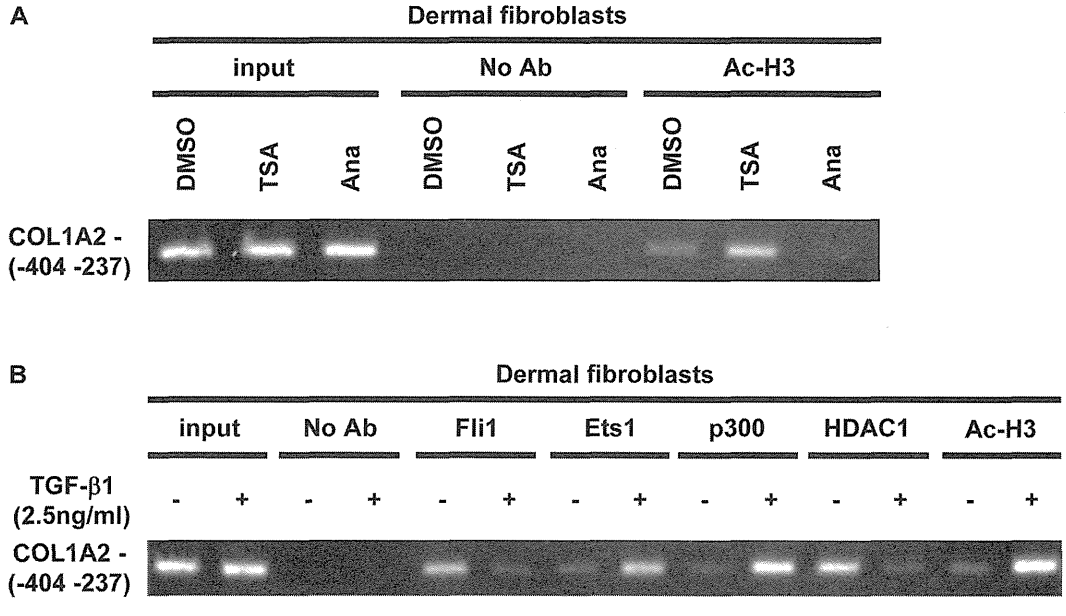

Figure 4. TGF-β-induced histone H3 acetylation correlates with Fli1/HDAC1 dissociation and Ets1/p300 recruitment to the COL1A2 promoter. A. Formaldehyde-cross-linked, moderately sheared chromatin was prepared from confluent quiescent fibroblasts treated with Trichostatin A (200 nM), anacardic acid (50 μM), or DMSO for 24 hours. The DNA fragments were immunoprecipitated using anti-acetylated histone H3 antibody, and the presence of the human α2(I) collagen (COL1A2) promoter fragments was detected using PCR. **B.** Formaldehyde-cross-linked, moderately sheared chromatin was prepared from foreskin fibroblasts untreated or treated with TGF-β1 (2.5 ng/ml) for 3 hours. The DNA fragments were immunoprecipitated using antibodies against Fli1, Ets1, p300, HDAC1, and acetylated histone H3. The presence of COL1A2 promoter fragments was detected using PCR.
doi:10.1371/journal.pone.0074930.g004

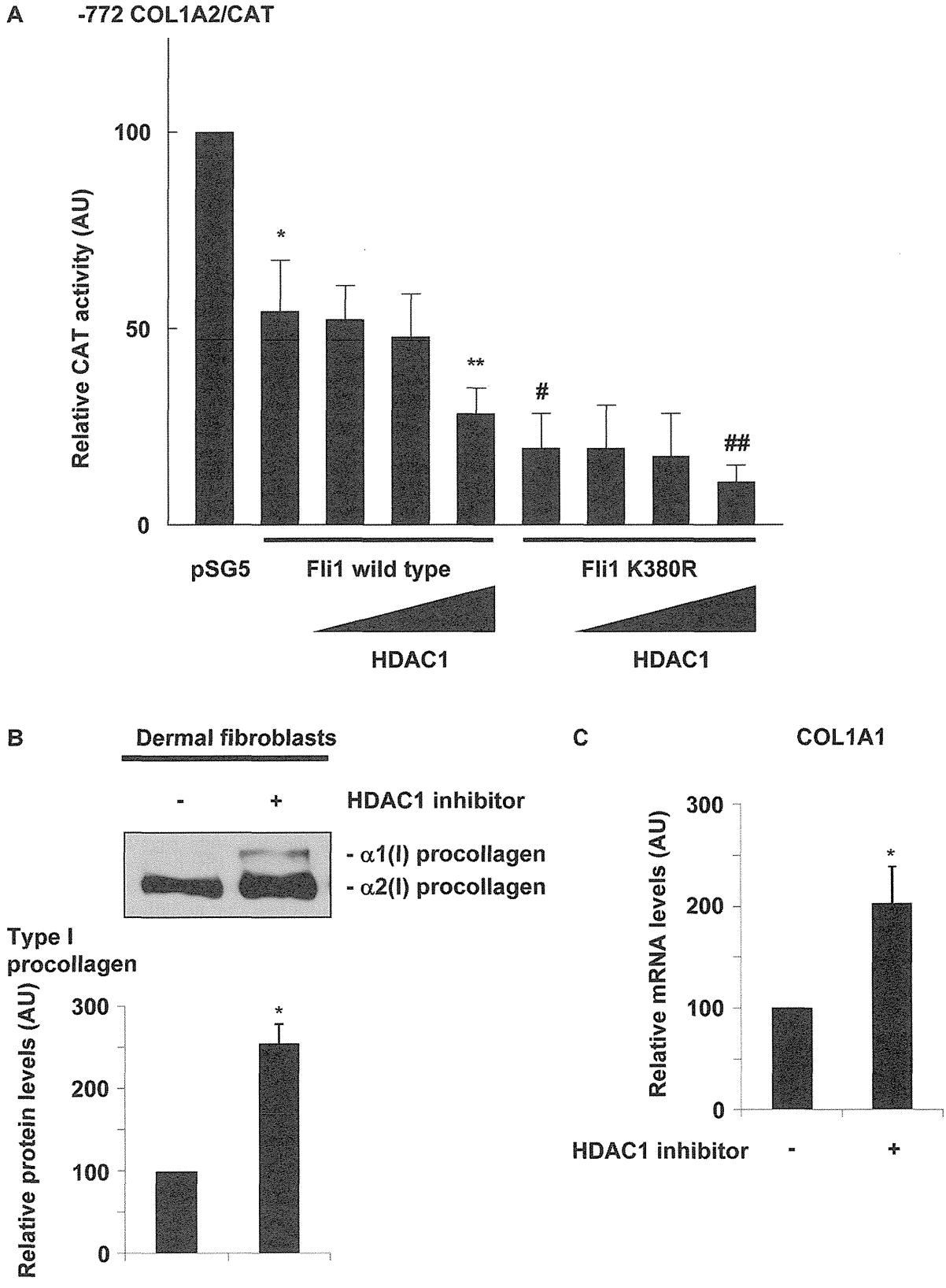

Figure 5. HDAC1 inhibits collagen gene expression in dermal fibroblasts. A. Foreskin fibroblasts were transfected with the −772 COL1A2/CAT construct (2 μg), along with wild type Fli1 or the Fli1 K380R mutant (0.1 μg) and HDAC1 (0, 0.1, 0.3, or 0.5 μg) for 48 h. Values represent CAT activities relative to those of untreated cells (100 arbitrary units [AU]). The mean and SD from three separate experiments are shown. * $p<0.05$ versus control cells. ** $p<0.05$ versus cells transfected with wild type Fli1 only. # $p<0.05$ versus control cells. ## $p<0.05$ versus cells transfected with Fli1 K380R only. **B.** Confluent quiescent foreskin fibroblasts were treated with HDAC1 inhibitor or vehicle for 24 hours. Type I procollagen protein levels in

whole cell lysates were determined by immunoblotting. A representative result of three independent experiments is shown. The band density was evaluated by densitometry. **C.** Under the same conditions, mRNA levels of the α1(I) collagen (COL1A1) gene were determined using reverse transcription quantitative real-time PCR. The graph represents -fold change in COL1A1 mRNA levels in comparison to unstimulated controls, which were arbitrarily set at 100. The mean and SD from three separate experiments are shown. * $p<0.05$ versus control cells treated with vehicle.
doi:10.1371/journal.pone.0074930.g005

In this study, we observed converse binding of Fli1 and Ets1 to the COL1A2 promoter *in vivo*. This confirms previous *in vitro* studies that showed competition of Ets1 and Fli1 for the Ets binding site on the COL1A2 promoter [10]. While Ets1 has been shown to be a positive mediator of fibrosis [18,25], its direct role in collagen gene regulation has not been fully defined, and surprisingly overexpression of Ets1 in dermal fibroblasts leads to inhibition of the COL1A2 gene [26]. Interestingly, recent ChIP-chip analysis of the Smad2/3 binding sites in HaCaT cells has revealed that the binding elements for Ets are significantly enriched in the Smad2/3 binding sites and knockdown of Ets1 results in overall alteration of TGF-β-induced transcription, suggesting that Ets contributes to the induction of the TGF-β-Smad pathways [27]. This global finding is consistent with earlier studies that showed cooperation of Ets1 and Smad3 on selected promoters, including the CCN2 gene [18]. Thus, it's possible that in the context of the COL1A2 promoter Ets1 functions as a partner of Smad3 contributing to the recruitment of p300/CBP and chromatin remodeling.

The key role of p300/CBP as a positive regulator of collagen gene expression has been well documented [28]. Interestingly, our study suggests that p300 also functions as a facilitator of complex formation between Fli1 and HDAC1 and contributes to the Fli1-mediated transcriptional inhibition of the COL1A2 gene. While counterintuitive, this observation is consistent with previous finding that demonstrated interaction of the C/H3 domain of p300 with HDAC1 *in vitro* and *in vivo* [29]. Functionally, it was shown that the recruitment of HDAC1 to the C/H3 domain interferes with the process of autoacetylation and the function of p300 as transcriptional co-activator of MyoD and p53. A HAT/HDAC complex is also involved in FOXP3-mediated transcriptional repression. Specifically, FOXP3 recruits histone acetyltransferase TIP60 and HDAC7 to form a repressor complex to control development and function of regulatory T cells [30]. While in the present study we did not characterize the additional components of the Fli1/HDAC1/p300 complexes, it is likely to be a part of a multiprotein complex that includes additional chromatin remodeling factors. Interestingly, a study that focused on PCAF has demonstrated formation of large multiprotein complexes that include both HATs and HDACs and are distinct from the HDAC complexes containing mSin3A, Mi-2/NRD, or CoREST [31]. The mechanism of transcriptional regulation by the HAT/HDAC complexes is not yet fully understood, and further studies are needed to better understand the role of these complexes in the process of dynamic chromatin remodeling in response to different physiological and pathological stimuli [32].

HDAC inhibitors have shown promise as therapeutic agents in several diseases including cancer, heart hypertrophy, and organ fibrosis [33]. With respect to dermal fibrosis, it was shown that the class I/II HDAC inhibitor, Trichostatin A, suppresses TGF-β-induced collagen up-regulation in scleroderma fibroblasts by interfering with Smad signaling [34]. A follow up study has revealed that specific blockade of HDAC7 reproduced the anti-fibrotic effects of Trichostatin A, however the mechanism involved in inhibition of collagen genes by silencing HDAC7 has not been elucidated [35]. Our study demonstrates that specific inhibition of HDAC1 has a pro-fibrotic effect, also in scleroderma fibroblasts (data not shown). Since downregulation of Fli1 may contribute to scleroderma fibrosis [12], it may not be desirable to employ class I HDAC inhibitors as an anti-fibrotic treatment for scleroderma. However, further studies are needed to gain a more comprehensive understanding of the effects of specific HDAC inhibitors on fibroblast function in physiological and pathological conditions for potential future applications as effective anti-fibrotic treatments.

In summary, this is the first study reporting the detailed molecular mechanism by which Fli1 functions as a potent transcriptional repressor in the context of the COL1A2 promoter. This finding provides us a new clue to further understand the

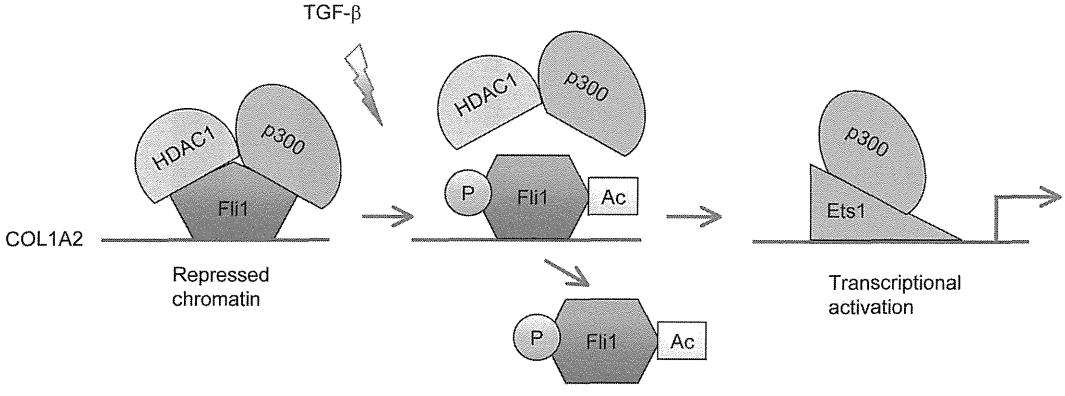

Figure 6. TGF-β-induced remodeling of the transcription factor complex at the Ets binding site in the human COL1A2 promoter. In quiescent cells, Fli1 forms a transcription repressor complex with p300 and HDAC1. HDAC1/p300 promotes deacetylation of Fli1, resulting in increased Fli1 DNA binding and a repressed chromatin state. After TGF-β stimulation, Fli1 phosphorylation by protein kinase C-δ induces disassembly of this transcription repressor complex and the acetylation of Fli1 by PCAF, leading to the loss of Fli1 DNA binding. Subsequently, the transcription activator complex consisting of Ets1 and p300 binds to the Ets binding site and activates transcription at least partially by promoting histone acetylation.
doi:10.1371/journal.pone.0074930.g006

molecular mechanism underlying Fli1-dependent transcriptional regulation of various target genes.

Acknowledgments

The authors wish to thank Dr. Bagrat Kapanadze for help with the proteomic analyses, and Paul Haines and Dr. Andreea Bujor for their help with the entinostat experiment.

References

1. Ben-David Y, Giddens EB, Bernstein A (1990) Identification and mapping of a common proviral integration site Fli-1 in erythroleukemia cells induced by Friend murine leukemia virus. Proc Natl Acad Sci U S A 87: 1332–1336.
2. Ben-David Y, Giddens EB, Letwin K, Bernstein A (1991) Erythroleukemia induction by Friend murine leukemia virus: insertional activation of a new member of the ets gene family, Fli-1, closely linked to c-ets-1. Genes Dev 5: 908–918.
3. Delattre O, Zucman J, Plougastel B, Desmaze C, Melot T, et al. (1992) Gene fusion with an ETS DNA-binding domain caused by chromosome translocation in human tumours. Nature 359: 162–165.
4. Hollenhorst PC, Jones DA, Graves BJ (2004) Expression profiles frame the promoter specificity dilemma of the ETS family of transcription factors. Nucleic Acids Res 32: 5693–5702.
5. Tamaki T, Ohnishi K, Hartl C, LeRoy EC, Trojanowska M (1995) Characterization of a GC-rich region containing Sp1 binding site(s) as a constitutive responsive element of the α2(I) collagen gene in human fibroblasts. J Biol Chem 270: 4299–4304.
6. Mager AM, Grapin-Botton A, Ladjali K, Meyer D, Wolff CM, et al. (1998) The avian fli gene is specifically expressed during embryogenesis in a subset of neural crest cells giving rise to mesenchyme. Int J Dev Biol 42: 561–572.
7. Masuya M, Moussa O, Abe T, Deguchi T, Higuchi T, et al. (2005) Dysregulation of granulocyte, erythrocyte, and NK cell lineages in Fli-1 gene-targeted mice. Blood 105: 95–102.
8. Spyropoulos DD, Pharr PN, Lavenburg KR, Jackers P, Papas TS, et al. (2000) Hemorrhage, impaired hematopoiesis, and lethality in mouse embryos carrying a targeted disruption of the Fli1 transcription factor. Mol Cell Biol 20: 5643–5652.
9. Asano Y, Stawski L, Hant F, Highland K, Silver R, et al. (2010) Endothelial Fli1 deficiency impairs vascular homeostasis: a role in scleroderma vasculopathy. Am J Pathol 176: 1983–1998.
10. Czuwara-Ladykowska J, Shirasaki F, Jackers P, Watson DK, Trojanowska M (2001) Fli-1 inhibits collagen type I production in dermal fibroblasts via an Sp1-dependent pathway. J Biol Chem 276: 20839–20848.
11. Jinnin M, Ihn H, Yamane K, Mimura Y, Asano Y, et al. (2005) α2(I) collagen gene regulation by protein kinase C signaling in human dermal fibroblasts. Nucleic Acids Res 33: 1337–1351.
12. Kubo M, Czuwara-Ladykowska J, Moussa O, Markiewicz M, Smith E, et al. (2003) Persistent down-regulation of Fli1, a suppressor of collagen transcription, in fibrotic scleroderma skin. Am J Pathol 163: 571–581.
13. Jinnin M, Ihn H, Asano Y, Yamane K, Trojanowska M, et al. (2006) Platelet derived growth factor induced tenascin-C transcription is phosphoinositide 3-kinase/Akt-dependent and mediated by Ets family transcription factors. J Cell Physiol 206: 718–727.
14. Shirasaki F, Makhluf HA, LeRoy C, Watson DK, Trojanowska M (1999) Ets transcription factors cooperate with Sp1 to activate the human tenascin-C promoter. Oncogene 18: 7755–7764.
15. Jinnin M, Ihn H, Mimura Y, Asano Y, Yamane K, et al. (2005) Matrix metalloproteinase-1 up-regulation by hepatocyte growth factor in human dermal fibroblasts via ERK signaling pathway involves Ets1 and Fli1. Nucleic Acids Res 33: 3540–3549.
16. Noda S, Asano Y, Akamata K, Aozasa N, Taniguchi T, et al. (2012) A possible contribution of altered cathepsin B expression to the development of skin sclerosis and vasculopathy in systemic sclerosis. PLoS One 7: e32272.
17. Noda S, Asano Y, Takahashi T, Akamata K, Aozasa N, et al. (2013) Decreased cathepsin V expression due to Fli1 deficiency contributes to the development of dermal fibrosis and proliferative vasculopathy in systemic sclerosis. Rheumatology (Oxford). [Epub ahead of print] PubMed PMID: 23287360.
18. Nakerakanti SS, Kapanadze B, Yamasaki M, Markiewicz M, Trojanowska M (2006) Fli1 and Ets1 have distinct roles in connective tissue growth factor/CCN2 gene regulation and induction of the profibrotic gene program. J Biol Chem 281: 25259–25269.
19. Noda S, Asano Y, Akamata K, Aozasa N, Taniguchi T, et al. (2012) Constitutive activation of c-Abl/protein kinase C-δ/Fli1 pathway in dermal fibroblasts derived from patients with localized scleroderma. Br J Dermatol 167: 1098–1105.
20. Asano Y, Czuwara J, Trojanowska M (2007) Transforming growth factor-β regulates DNA binding activity of transcription factor Fli1 by p300/CREB-binding protein-associated factor-dependent acetylation. J Biol Chem 282: 34672–34683.
21. Asano Y, Trojanowska M (2009) Phosphorylation of Fli1 at threonine 312 by protein kinase C δ promotes its interaction with p300/CREB-binding protein-associated factor and subsequent acetylation in response to transforming growth factor β. Mol Cell Biol 29: 1882–1894.
22. Bujor AM, Asano Y, Haines P, Lafyatis R, Trojanowska M (2011) The c-Abl tyrosine kinase controls protein kinase Cδ-induced Fli-1 phosphorylation in human dermal fibroblasts. Arthritis Rheum 63: 1729–1737.
23. Nakerakanti SS, Kapanadze B, Yamasaki M, Markiewicz M, Trojanowska M (2006) Fli1 and Ets1 have distinct roles in connective tissue growth factor/CCN2 gene regulation and induction of the profibrotic gene program. J Biol Chem 281: 25259–25269.
24. Fournel M, Bonfils C, Hou Y, Yan PT, Trachy-Bourget MC, et al. (2008) MGCD0103, a novel isotype-selective histone deacetylase inhibitor, has broad spectrum antitumor activity in vitro and in vivo. Mol Cancer Ther 7: 759–768.
25. Baran CP, Fischer SN, Nuovo GJ, Kabbout MN, Hitchcock CL, et al. The transcription factor ets-2 plays an important role in the pathogenesis of pulmonary fibrosis. Am J Respir Cell Mol Biol. 45: 999–1006.
26. Czuwara-Ladykowska J, Sementchenko VI, Watson DK, Trojanowska M (2002) Ets1 is an effector of the transforming growth factor β (TGF-β) signaling pathway and an antagonist of the profibrotic effects of TGF-β. J Biol Chem 277: 20399–20408.
27. Koinuma D, Tsutsumi S, Kamimura N, Taniguchi H, Miyazawa K, et al. (2009) Chromatin immunoprecipitation on microarray analysis of Smad2/3 binding sites reveals roles of ETS1 and TFAP2A in transforming growth factor β signaling. Mol Cell Biol 29: 172–186.
28. Ghosh AK, Varga J (2007) The transcriptional coactivator and acetyltransferase p300 in fibroblast biology and fibrosis. J Cell Physiol 213: 663–671.
29. Simone C, Stiegler P, Forcales SV, Bagella L, De Luca A, et al. (2004) Deacetylase recruitment by the C/H3 domain of the acetyltransferase p300. Oncogene 23: 2177–2187.
30. Li B, Samanta A, Song X, Iacono KT, Bembas K, et al. (2007) FOXP3 interactions with histone acetyltransferase and class II histone deacetylases are required for repression. Proc Natl Acad Sci U S A 104: 4571–4576.
31. Yamagoe S, Kanno T, Kanno Y, Sasaki S, Siegel RM, et al. (2003) Interaction of histone acetylases and deacetylases in vivo. Mol Cell Biol 23: 1025–1033.
32. Pesenico A, Simone C (2011) Physical and functional HAT/HDAC interplay regulates protein acetylation balance. J Biomed Biotechnol 2011: 371832.
33. Pang M, Zhuang S (2010) Histone deacetylase: a potential therapeutic target for fibrotic disorders. J Pharmacol Exp Ther 335: 266–272.
34. Huber LC, Distler JH, Moritz F, Hemmatazad H, Hauser T, et al. (2007) Trichostatin A prevents the accumulation of extracellular matrix in a mouse model of bleomycin-induced skin fibrosis. Arthritis Rheum 56: 2755–2764.
35. Hemmatazad H, Rodrigues HM, Maurer B, Brentano F, Pileckyte M, et al. (2009) Histone deacetylase 7, a potential target for the antifibrotic treatment of systemic sclerosis. Arthritis Rheum 60: 1519–1529.

Author Contributions

Conceived and designed the experiments: YA MT. Performed the experiments: YA. Analyzed the data: YA MT. Contributed reagents/materials/analysis tools: YA. Wrote the paper: YA MT.

RHEUMATOLOGY

Rheumatology 2013;52:1239–1244
doi:10.1093/rheumatology/ket010
Advance Access publication 26 February 2013

Concise report

A possible contribution of visfatin to the resolution of skin sclerosis in patients with diffuse cutaneous systemic sclerosis via a direct anti-fibrotic effect on dermal fibroblasts and Th1 polarization of the immune response

Yuri Masui[1], Yoshihide Asano[1], Sayaka Shibata[1], Shinji Noda[1], Kaname Akamata[1], Naohiko Aozasa[1], Takashi Taniguchi[1], Takehiro Takahashi[1], Yohei Ichimura[1], Tetsuo Toyama[1], Hayakazu Sumida[1], Koichi Yanaba[1], Yayoi Tada[1], Makoto Sugaya[1], Shinichi Sato[1] and Takafumi Kadono[1]

Abstract

Objective. Visfatin is a member of the adipocytokines with pro-fibrotic, pro-inflammatory and immunomodulating properties potentially implicated in the pathogenesis of certain fibrotic and inflammatory autoimmune diseases. In this study, we investigated the clinical significance of serum visfatin levels and its contribution to the developmental process in SSc.

Methods. Serum visfatin levels were determined by a specific ELISA in 57 SSc patients and 19 healthy controls. The mRNA levels of target genes were determined in normal and SSc fibroblasts by real-time RT-PCR. The levels of IL-12p70 produced by THP-1 cells were measured by a specific ELISA.

Results. Serum visfatin levels were comparable among total SSc, diffuse cutaneous SSc (dcSSc), limited cutaneous SSc and healthy controls. The only finding in a series of analyses regarding the correlation of serum visfatin levels with clinical symptoms and laboratory data was the significantly longer disease duration in dcSSc with elevated serum visfatin levels than in those with normal levels. Consistently, serum visfatin levels were significantly elevated in late-stage dcSSc (disease duration >6 years), but not in early and mid-stage dcSSc compared with healthy controls. In *in vitro* experiments, visfatin reversed the pro-fibrotic phenotype of SSc dermal fibroblasts and induced the expression of IL-12p70 in THP-1 cells treated with IFN-γ plus lipopolysaccharide.

Conclusion. Visfatin may contribute to the resolution of skin sclerosis in late-stage dcSSc via a direct anti-fibrotic effect on dermal fibroblasts and Th1 polarization of the immune response.

Key words: systemic sclerosis, visfatin, collagen, matrix metalloproteinase 1, interleukin-12.

CLINICAL

Introduction

SSc is a multisystem autoimmune disease characterized by vascular injuries and fibrosis of skin and certain internal organs. Although the pathogenesis of SSc remains unknown, our latest studies disclosed a possible contribution of adipocytokines to the pathological process of SSc [1].

Visfatin is a member of the adipocytokines, which are key regulators of metabolism and insulin resistance [2]. Emerging evidence has demonstrated that some adipocytokines have pro- or anti-fibrotic, pro- or anti-inflammatory and immunomodulating properties [3–6]. Visfatin is ubiquitously expressed in different cell types, including adipocytes, macrophages and lymphocytes. Reflecting

[1]Department of Dermatology, University of Tokyo Graduate School of Medicine, Tokyo, Japan.

Submitted 19 May 2012; revised version accepted 18 January 2013.

Correspondence to: Yoshihide Asano, Department of Dermatology, University of Tokyo Graduate School of Medicine, 7-3-1 Hongo, Bunkyo-ku, Tokyo 113-8655, Japan. E-mail: yasano-tky@umin.ac.jp

its pro-inflammatory properties, visfatin is up-regulated in adequate inflammatory conditions, including models of acute lung injury and clinical and experimental sepsis [7]. On the other hand, visfatin appears to be involved in the pathological process of inflammatory autoimmune diseases, including RA, Behçet's disease (BD) and IBD [8, 9]. Regarding SSc, despite the potential role of visfatin in cardiac and hepatic fibrosis [4–6], a previous report revealed that serum visfatin levels are comparable between patients and healthy controls [9], suggesting a small role of visfatin in the pathological process of SSc. However, since SSc is a heterogeneous disease consisting of certain disease subsets, including diffuse cutaneous SSc (dcSSc) and limited cutaneous SSc (lcSSc), this study was conducted to precisely evaluate the significance of visfatin in the pathological process of SSc.

Materials and methods

Patients

Serum samples, frozen at −80°C until assayed, were obtained from 57 SSc patients (55 women, 2 men) and 19 healthy individuals (18 women, 1 man). Patients treated with corticosteroids or other immunosuppressants prior to their first visits were excluded. Patients were grouped by the LeRoy classification system [10]: 28 patients with lcSSc and 29 with dcSSc. All dcSSc and 23 lcSSc patients fulfilled the criteria proposed by the ACR [11]. Five lcSSc patients not meeting these criteria had sclerodactyly and at least two of the following features: calcinosis, RP, esophageal dysmotility and telangiectasia. The study was performed according to the Declaration of Helsinki and approved by the ethical committee of the University of Tokyo Graduate School of Medicine.

Measurement of serum visfatin levels

Specific ELISA kits (Phoenix Pharmaceuticals, Belmont, CA, USA) were used to measure serum visfatin levels (analytical range 0.1–1000 ng/ml) according to the manufacturer's instructions without any modification. Polystyrene 96-well plates coated with anti-visfatin antibodies were incubated with diluted sera, then washed and incubated with horseradish peroxidase-conjugated anti-visfatin antibodies. The wells were washed again, tetramethylbenzidine was added and then the wells were incubated. Finally, sulphuric acid was added to terminate the reaction and the absorbance at 450 nm was measured. Serum visfatin levels were calculated using a standard curve.

Clinical assessments

The clinical and laboratory data were obtained when the blood samples were drawn. Disease duration was defined as the interval between the onset, defined as the first clinical event of SSc other than RP, and the time the blood samples were drawn. The details of assessments for clinical symptoms are briefly summarized in the legends of supplementary Table S1, available at *Rheumatology* Online.

Cell cultures

Dermal fibroblasts were obtained by skin biopsy from the affected areas (dorsal forearm) of five dcSSc patients with <2 years of skin thickening (skin score of biopsy site: 3 for two patients, 2 for one patient and 1 for the others) and from the corresponding areas of five closely matched healthy donors. THP-1 cells were purchased from American Tissue Culture Collection (Rockville, MA, USA).

RNA isolation and real-time RT-PCR

RNA isolation and real-time RT-PCR were carried out as described previously [12]. The sequences of human α2(I) collagen (COL1A2), MMP-1 and 18S rRNA primers are summarized in supplementary Table S2, available at *Rheumatology* Online.

Measurement of IL-12p70 production by THP-1 cells

The production of IL-12p70 from THP-1 cells was analysed by a specific ELISA kit (BD Pharmingen, San Diego, CA, USA) using the cell culture media following the manufacturer's specifications with minor modification. We diluted standard samples and confirmed the complete correlation of IL-12p70 concentrations with the OD 595 nm light absorption values between 0.488 pg/ml and 125 ng/ml ($R^2 = 0.9998$).

Statistical analysis

The statistical analysis was carried out with a Kruskal–Wallis test and a Steel–Dwass test for multiple comparison and with Mann–Whitney *U* test for two-group comparison. Correlations with clinical data were assessed by Spearman's rank correlation coefficient. Statistical significance was defined as a *P*-value <0.05.

Results

Serum visfatin levels and their clinical correlation in SSc

There was no difference in serum visfatin levels among total SSc, dcSSc, lcSSc and healthy controls (Fig. 1A). Given that there was a subset of SSc patients with increased serum visfatin levels (above dotted line in Fig. 1A), especially in dcSSc, serum visfatin levels potentially reflect some aspect of disease process in SSc.

We next evaluated the correlation of serum visfatin levels with parameters reflecting dermal and pulmonary fibrosis, such as modified Rodnan total skin thickness score, the percentage of predicted vital capacity and the percentage of predicted diffusion lung capacity for carbon monoxide, in dcSSc, lcSSc and dcSSc with disease duration <6 years in which fibrotic response is extensively active. No significant correlation was detected (data not shown). For further analyses, SSc patients were classified into two groups according to cut-off value [mean + 2 S.D. (10.60 ng/ml) of controls, which is normally distributed]. Clinical features, other than skin sclerosis and interstitial lung disease, of SSc patients with elevated or normal serum visfatin levels were evaluated in dcSSc and lcSSc (supplementary Table S1, available at *Rheumatology*

FIG. 1 Concentrations of visfatin in sera from patients with SSc and healthy individuals.

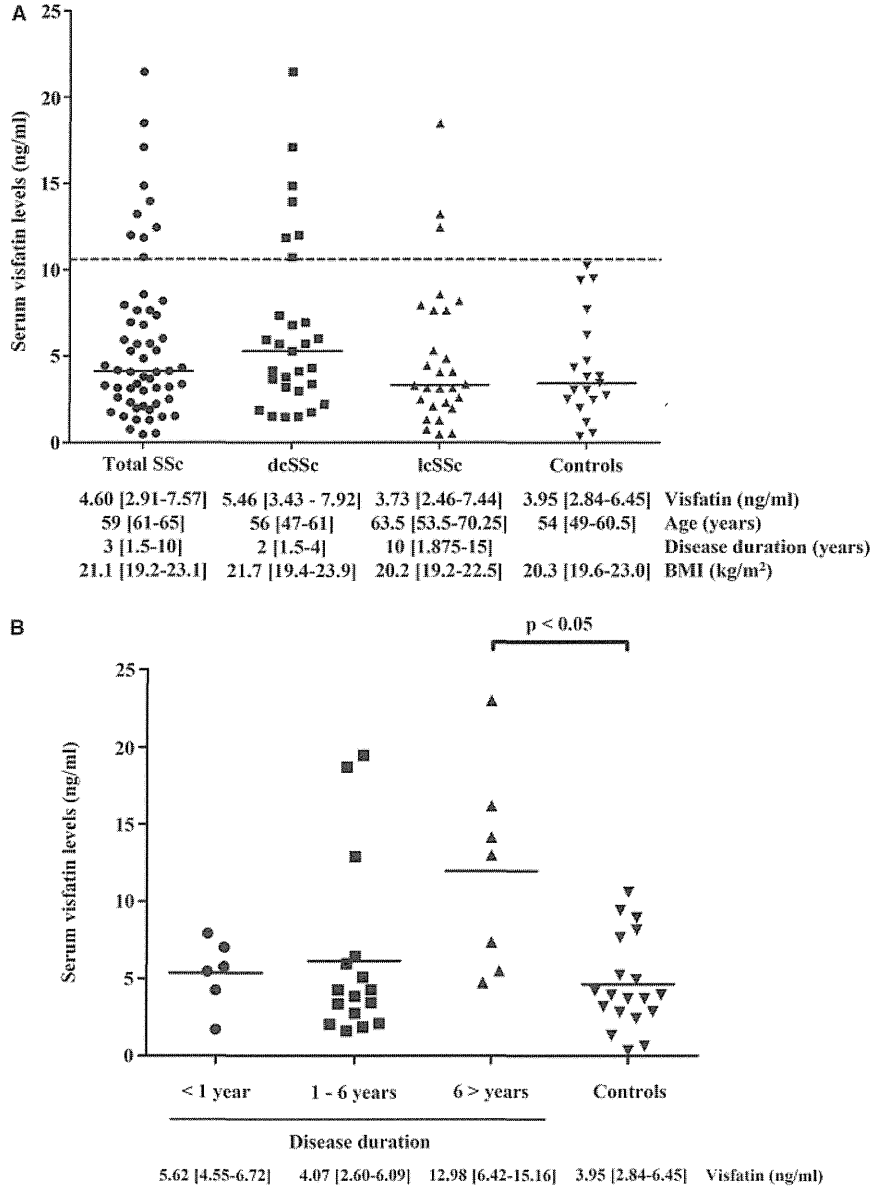

Serum visfatin levels were determined by a specific ELISA in SSc patients and healthy controls. The levels were compared among total SSc, dcSSc, lcSSc and healthy controls (**A**). dcSSc patients were divided into three subgroups, including those with disease duration of <1 year, those with disease duration 1–6 years and those with disease duration >6 years, and further analysed (**B**). The horizontal bars indicate the median value in each group. A dotted line represents a cut-off value (mean + 2 S.D. of healthy controls). The values below the graphs represent median values (25th–75th percentile) of serum visfatin levels, age, disease duration and BMI in each patient group. The statistical analysis was carried out with a Kruskal–Wallis test and a Steel–Dwass test. Statistical significance was defined as a *P*-value <0.05.

Online). There was no significant difference between these groups in terms of sex or age of onset, while disease duration was significantly longer in patients with elevated serum visfatin levels than in those with normal levels among dcSSc [7 years (2.3–14.5) *vs* 2 years (1.1–3)], but not among lcSSc. Regarding other symptoms, the prevalence of each was comparable between the two groups in dcSSc and lcSSc. Although visfatin is a pro-inflammatory cytokine [3], the levels of high-sensitivity CRP and ESR did not correlate with serum visfatin levels in dcSSc, dcSSc with disease duration <6 years and lcSSc (data not shown). Collectively, serum visfatin levels are

barely associated with any clinical features, except for disease duration, in SSc.

Increase in serum visfatin levels along with disease duration in dcSSc

We further classified dcSSc patients into three subgroups according to their disease duration: early dcSSc (disease duration <1 year), mid-stage dcSSc (disease duration 1–6 years) and late-stage dcSSc (disease duration >6 years), and evaluated the correlation of serum visfatin levels with disease stage. As shown in Fig. 1B, the multiple comparison analysis showed the significant difference between late-stage dcSSc and healthy controls, suggesting that visfatin contributes to certain pathological processes in late-stage dcSSc.

Visfatin exerted an anti-fibrotic effect on SSc dermal fibroblasts and increased IL-12p70 production in THP-1 cells

Late-stage dcSSc is generally characterized by the spontaneous resolution of skin sclerosis, suggesting that visfatin has an anti-fibrotic effect on SSc dermal fibroblasts. Therefore we investigated the effect of visfatin on the COL1A2 and MMP-1 mRNA levels in normal and SSc dermal fibroblasts. Consistent with previous reports [13, 14], COL1A2 mRNA levels significantly increased in SSc dermal fibroblasts compared with normal dermal fibroblasts, while MMP-1 mRNA levels were comparable between them (Fig. 2A), indicating that dermal fibroblasts from patients maintain SSc phenotype. Therefore the following experiments were carried out by using these cells. In SSc dermal fibroblasts, expectedly, visfatin suppressed COL1A2 mRNA expression, while increasing MMP-1 mRNA levels, in a dose-dependent manner. In contrast, visfatin did not affect the COL1A2 and MMP-1 mRNA levels in normal dermal fibroblasts. These results were also confirmed at protein levels by immunoblotting (Fig. 2B and C). Importantly, visfatin also reversed the pro-fibrotic phenotype of normal dermal fibroblasts stimulated with transforming growth factor β1 (supplementary Fig. S1, available at *Rheumatology* Online). Collectively visfatin exerts an anti-fibrotic effect on activated dermal fibroblasts with the pro-fibrotic phenotype.

Given that immune polarization in dcSSc generally shifts from T helper 2 (Th2) to T helper 1 (Th1) along with disease course [15], the elevation of visfatin in late-stage dcSSc suggests that visfatin promotes Th1 polarization of the immune response. Supporting this, visfatin induced the up-regulated expression of IL-12p70 in THP-1 cells differentiated with IFN-γ and lipopolysaccharide (LPS) (Fig. 2D). Thus visfatin-dependent Th1 immune polarization may contribute to the skin resolution in late-stage dcSSc.

Discussion

The present study provided the following new findings: (i) disease duration is significantly longer in dcSSc with elevated serum visfatin levels than in those with normal levels; (ii) serum visfatin levels are comparable to normal levels during early- and mid-stage dcSSc, but are significantly increased in late-stage dcSSc and (iii) visfatin exerts an anti-fibrotic effect on SSc dermal fibroblasts and is likely to skew toward Th1 immune responses. These suggest that the elevation of visfatin is involved in the mechanism explaining the resolution of skin sclerosis in late-stage dcSSc.

The immunomodulating property of visfatin has been well studied in RA and its animal models. In addition to high visfatin levels in plasma, serum and SF in RA [16, 17], visfatin gene expression is increased in synovial tissue from RA [17, 18] and in inflamed synovial tissue of mice with collagen-induced arthritis [18]. Importantly, pharmacological inhibition of visfatin significantly reduces inflammation, cartilage damage and the severity of arthritis with comparable activity to TNF inhibitors in a collagen-induced arthritis model [19]. Supporting this, an inhibitor of visfatin decreases the production of TNF-α and IL-6 by murine peritoneal exudate inflammatory cells and human monocytes *in vitro* [19]. Similar to RA, circulating visfatin levels are elevated and positively correlate with disease activity in BD [3, 9]. Given that RA and BD are characterized by Th1 polarization of Th immune response, visfatin may contribute to Th1 immune polarization in the active stage of these diseases. Since immune polarization in SSc generally shifts from Th2 to Th1 in parallel with disease duration [15], the present serum data, together with previous data in RA and BD, suggest that visfatin contributes to the resolution of skin sclerosis by promoting Th1 immune polarization in concert with various cytokines in SSc. Consistent with our hypothesis, visfatin increased the production of IL-12p70 in THP-1 cells differentiated with IFN-γ and LPS. Collectively visfatin may contribute to the resolution of skin sclerosis at least partially by promoting the Th1 immune polarization in late-stage dcSSc.

Another novel finding in this study was that visfatin elicits an anti-fibrotic effect on SSc dermal fibroblasts. The effect of visfatin on fibrosis has been well studied in a couple of fibrotic disorders. Serum visfatin levels correlate with fibrosis scores in patients with chronic hepatitis C [4] and visfatin expression is positively associated with fibrosis stage in non-alcoholic fatty liver disease [5]. Supporting this, visfatin induces the expression of basic fibroblast growth factor in rat hepatic stellate cells [20]. Furthermore, visfatin promotes the proliferation and the synthesis of type I and type III collagen in rat cardiac fibroblasts [6]. Thus visfatin is potentially associated with the development and progression of fibrotic condition in cardiac and liver fibrosis. Taken together with these previous data, our present observation suggests that visfatin has a dual effect on fibrosis in a context-dependent manner. Although the detailed mechanism by which visfatin reverses the pro-fibrotic phenotype in SSc fibroblasts remains unknown, visfatin coordinately promotes the resolution of skin sclerosis in late-stage dcSSc by inhibiting the pro-fibrotic phenotype of SSc dermal fibroblasts and driving Th1 polarization.

FIG. 2 The effect of visfatin on the levels of type I collagen and MMP-1 in normal and SSc dermal fibroblasts and on IL-12p70 production in THP-1 cells.

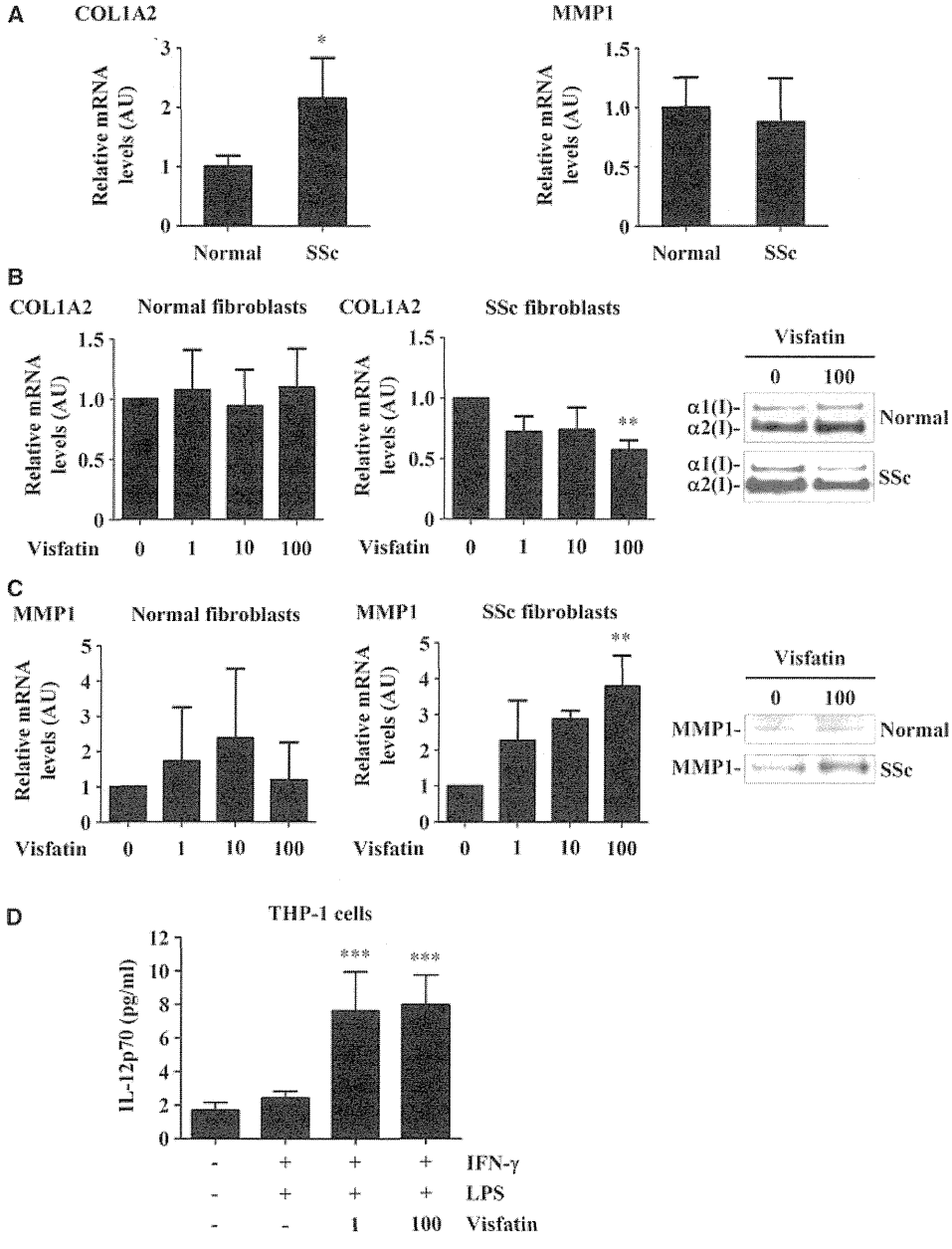

Subconfluent normal and SSc dermal fibroblasts were serum starved for 24 h, then the cell culture medium was refreshed and cells were stimulated with the indicated concentration of visfatin (PeprTech, Rocky Hill, NJ, USA) for another 24 h. mRNA levels of human α2(I) collagen (COL1A2) and MMP-1 genes were determined by real-time RT-PCR under a quiescent condition (**A**) or after the treatment with the indicated concentration of visfatin (**B**, **C**). The levels of type I collagen [α1(I) collagen (α1(I)) and α2(I) collagen (α2(I))] and MMP-1 proteins in the culture media were also determined by immunoblotting using anti-type I collagen antibody (Southern Biotech, Birmingham, AL, USA) and anti-MMP-1 antibody (Millipore, Billerica, MA, USA). The volume of each medium sample analysed was normalized based on cell number. THP-1 cells in the log phase of growth were primed with 100 ng/ml IFN-γ (R&D Systems, Minneapolis, MN, USA) for 6 h and stimulated with 100 ng/ml LPS (InvivoGen, San Diego, CA, USA) in the presence or absence of visfatin. Sixteen hours after treatment, the levels of IL-12p70 in each supernatant were analysed by a specific ELISA kit (**D**). The statistical analysis was carried out with Mann–Whitney *U* test for two-group comparison and with a Kruskal–Wallis test and a Steel–Dwass test for multiple comparison. **P* <0.05 versus normal dermal fibroblasts. ***P* <0.05 versus SSc dermal fibroblasts without visfatin stimulation. ****P* <0.05 versus THP-1 cells without any stimulation and those treated with IFN-γ and LPS.